

APOPTOTIC CELLS ACTIVATE AMPK AND INHIBIT EPITHELIAL CELL GROWTH WITHOUT CHANGE IN INTRACELLULAR ENERGY STORES*

Vimal A. Patel^{†,§,1,2}, Donald Massenburg^{†,§,1}, Snezana Vujicic^{†,§}, Lanfei Feng^{†,§}, Meiyi Tang^{¶,§}, Natalia Litbarg^{†,§}, Angelika Antoni[‡], Joyce Rauch[‡], Wilfred Lieberthal^{¶,§,3}, and Jerrold S. Levine^{†,‡,§,3}

[†]From the Section of Nephrology, Department of Medicine, and the [‡]Department of Microbiology and Immunology, University of Illinois, Chicago, Illinois 60612, the [§]Section of Nephrology, Department of Medicine, Jesse Brown Veterans Affairs Hospital, Chicago, Illinois 60612, the [¶]Section of Nephrology, Department of Medicine, Stony Brook University Medical Center, Stony Brook, New York 11794, the [#]Northport Veterans Affairs Hospital, Northport, New York 11768, the [‡]Department of Biology, Kutztown University of Pennsylvania, Kutztown, Pennsylvania 19530, and the [‡]Division of Rheumatology, Department of Medicine, Research Institute of the McGill University Health Centre, Montreal, Quebec H4A 3J1, Canada

*Running title: Apoptotic cells activate AMPK and inhibit cell growth

¹These authors contributed equally to this work.

²Present address: NorthShore Neurological Institute, NorthShore University HealthSystem, Pritzker School of Medicine, Evanston, Illinois 60201.

³These authors contributed equally to this work.

To whom correspondence and reprint requests should be addressed: Jerrold S. Levine, Section of Nephrology, Dept. of Medicine, University of Illinois at Chicago, 840 South Wood Street, MC-793, Chicago, IL 60612. Tel.: 312-413- 1178; Fax: 312-996-7378; E-mail: jslevine@uic.edu.

Keywords: Apoptosis, Epithelial cell, Innate immunity, Cell growth, AMP, ADP, ATP, AMP-activated kinase (AMPK), Kidney, Akt/ PKB

The abbreviations used are: AMPK, AMP-activated protein kinase; BU.MPT, Boston University mouse proximal tubule; CaMKK β , Ca²⁺/calmodulin-activated protein kinase kinase β ; CC, compound C; GSK, glycogen synthase kinase; m ϕ , macrophages; LC/MS/MS, liquid chromatography-tandem mass spectrometry; LKB1, liver kinase B1; mTORC1, mammalian target of rapamycin complex 1; m/z, mass-to-charge ratio; p70S6K, p70 S6 kinases 1 and 2; PDK1, 3-phosphoinositide-dependent protein kinase 1; PKA, protein kinase A; PI, propidium iodide; PTEC, proximal tubular epithelial cell; S6, S6 ribosomal protein; TSC, tuberous sclerosis complex

Background: Non-professional phagocytes, like epithelial cells, recognize apoptotic cells.

Results: Apoptotic cells mimic the effects of intracellular energy depletion and inhibit the growth (cell size) of epithelial cells with which they interact.

Conclusion: Apoptotic cells activate AMP-activated protein kinase (AMPK) and inhibit cell growth.

Significance: By acting as sentinels of environmental stress, apoptotic targets enable nearby cells to monitor and adapt to local change.

ABSTRACT

Apoptosis plays an indispensable role in the maintenance and development of tissues. We

have shown that receptor-mediated recognition of apoptotic target cells by viable kidney proximal tubular epithelial cells (PTECs) inhibits the proliferation and survival of PTECs. Here, we examined the effect of apoptotic targets on PTEC cell growth (cell size during G1 phase of cell cycle). Using a cell culture model, we show that apoptotic cells potentially activate AMP-activated protein kinase (AMPK), a highly sensitive sensor of intracellular energy stores. AMPK activation leads to decreased activity of its downstream target, ribosomal protein p70 S6 kinase (p70S6K) and concomitant inhibition of cell growth. Importantly, these events occur without detectable change in intracellular levels of AMP, ADP, or ATP. Inhibition of AMPK, either pharmacologically by compound C or molecularly by shRNA, diminishes the effects of apoptotic targets, and largely restores p70S6K activity and cell size to normal levels. Apoptotic targets also inhibit Akt, a second signaling pathway regulating cell growth. Expression of a constitutively active Akt construct partially relieved cell growth inhibition, but was less effective than inhibition of AMPK. Inhibition of cell growth by apoptotic targets is dependent on physical interaction between apoptotic targets and PTECs, but independent of phagocytosis. We conclude that receptor-mediated recognition of apoptotic targets mimics the effects of intracellular energy depletion, activating AMPK and inhibiting cell growth. By acting as sentinels of environmental change, apoptotic death may enable nearby viable cells, especially non-migratory epithelial cells, to monitor and adapt to local stresses.

Apoptosis plays an indispensable role in the maintenance and development of tissues. At the most straightforward level, apoptosis provides a means for the rapid and efficient removal of aged, damaged, or excess cells without harm to surrounding tissues (1, 2). In addition to this essentially passive activity, apoptosis also contributes in a more dynamic manner to tissue homeostasis. Cells dying by apoptosis acquire multiple new activities, both secreted and cell-associated, that allow them to modulate the

function of nearby live cells (3-9). While earlier studies focused on the ability of apoptotic cells to suppress inflammation (10-15), apoptotic cells also affect a broad range of cellular functions, including such vital activities as survival (3, 8, 9), proliferation (3, 8, 9), differentiation (16), and migration (17). Moreover, these effects are not limited to professional phagocytes, like macrophages (m ϕ), but extend to virtually all cell types and lineages, including traditionally non-phagocytic cells, such as epithelial and endothelial cells (6, 8, 9, 17, 18).

Importantly, the specific effects elicited in nearby viable cells following exposure to apoptotic cells depend on multiple factors relating both to the viable responding cells and to the apoptotic cell itself. For example, while the responses by murine m ϕ and kidney proximal tubular epithelial cells (PTECs) are similar with respect to proliferation, with inhibition of proliferation occurring in both cases, the responses of these two cells differ with respect to survival (3, 5, 8, 9). Apoptotic cells promote m ϕ survival, whereas they induce the apoptotic death of PTECs (3, 5, 8, 9). Even for responding cells of the same lineage, responses can differ depending on their organ of origin (e.g., PTECs versus mammary epithelial cells) (9) or state of activation (e.g., neutrophils) (20). Conversely, apoptotic cells may evoke different responses in the same cell depending on the nature of the apoptotic stimulus (9, 21) or the time elapsed from administration of the apoptotic stimulus to interaction between apoptotic and responding cells (9, 13).

In light of this complexity, it is interesting to speculate about the *in vivo* consequences of a local increase in apoptotic death. As we have previously hypothesized (9, 22), such an increase may serve as a signal of environmental change or stress. A tissue's overall response, comprising the integrated responses of its component cells, may then represent an attempt at adaptation. A physiologically relevant example would be the vasoconstriction or partial occlusion of an artery supplying a segment of an organ such as the kidney. This will lead to a reduced delivery of oxygen and nutrients. Within the affected zone, the response of individual viable cells to nearby dead or dying target cells will depend on the responding cell's lineage and anatomic location, among other factors, both intrinsic and extrinsic.

Some cells, such as infiltrating mφ, will demonstrate increased survival, reflecting their importance in clearance of debris and repair (3, 5). Other cells, in contrast, such as kidney PTECs, will evince decreased proliferation and survival, reflecting the need to decrease metabolic demand in the face of reduced supply (8, 9).

AMP-activated protein kinase (AMPK) is a highly sensitive sensor of intracellular energy stores (23, 24). Activation of AMPK occurs primarily as a result of an increase in the ratio of either AMP or ADP to ATP (23, 25). Upon activation, AMPK acts as a metabolic switch with profound effects on intermediary cell metabolism. The net outcome is the augmentation or conservation of intracellular energy stores, through promotion of ATP production, inhibition of ATP consumption, and facilitated cellular uptake of nutrients (23, 24). A major downstream target of AMPK is the mammalian target of rapamycin complex 1 (mTORC1), a kinase critical for cell growth (increase of cell mass) and proliferation (increase of cell number) (23, 24, 26-29). Inhibition of mTORC1 by AMPK leads to inhibition of cell growth, and thereby cell size, by preventing mTORC1-mediated phosphorylation and activation of the ribosomal proteins p70 S6 kinases 1 and 2 (p70S6K) (27-29).

Here, using a cell culture model, we test the hypothesis that exposure of murine kidney PTECs to apoptotic target cells acts as an extracellular stress, mimicking the effects of intracellular depletion of energy stores. We show that apoptotic targets potently activate AMPK, leading to decreased activity of p70S6K and concomitant inhibition of cell growth. Importantly, these events occur without detectable change in intracellular energy stores. Inhibition of AMPK, either pharmacologically by compound C or molecularly by shRNA, diminishes the effects of apoptotic targets, and largely restores p70S6K activity and cell size to normal levels. Together with our previous results, our data reveal that apoptotic cells inhibit the growth and proliferation of nearby PTECs responders. By acting as sentinels of environmental change, apoptotic death may allow nearby viable cells, especially non-migratory epithelial cells, to monitor and adapt to local stresses.

EXPERIMENTAL PROCEDURES

Materials—Unless otherwise stated, all chemicals were obtained from Sigma (St. Louis, MO), Invitrogen (Carlsbad, CA), or Fisher Scientific (Pittsburgh, PA). Cell culture medium was obtained from Mediatech (Herndon, VA).

Antibodies—Affinity-purified polyclonal rabbit antibodies detecting the active Thr¹⁷²-phosphorylated forms of α1-AMPK and α2-AMPK, the Thr³⁰⁸-phosphorylated form of Akt, the Ser⁴⁷³-phosphorylated form of Akt, total p70S6K1 and p70S6K2, the active Thr³⁸⁹-phosphorylated form of p70S6K1 and p70S6K2, the active Ser^{240/244}-phosphorylated form of S6 ribosomal protein, the active Thr²⁴-phosphorylated form of FoxO1, the active Thr³²-phosphorylated form of FoxO3a, the inactive Ser²¹-phosphorylated form of glycogen synthase kinase (GSK) 3α, the inactive Ser⁹-phosphorylated form of GSK3β, and total β-actin were obtained from Cell Signaling Technology (Beverly, MA). Rabbit mAb (57C12) detecting total β1-AMPK and β2-AMPK and rabbit mAb (14C10) detecting total GAPDH were obtained from Cell Signaling Technology. Horseradish peroxidase-linked donkey anti-rabbit F(ab')₂ from GE Healthcare Bio-Sciences (Pittsburgh, PA) was used as a secondary antibody for detection of western blots by enhanced chemiluminescence.

Cell Culture—All cells were grown at 37°C in a humidified 5% (v/v) CO₂ atmosphere unless otherwise stated. The conditionally immortalized mouse kidney PTEC cell line (BU.MPT, Boston University mouse proximal tubule) was maintained in high-glucose DMEM medium containing 10% (v/v) heat-inactivated FBS, 2 mM L-glutamine, 10 mM HEPES, 100 U/ml penicillin-streptomycin, and 10 U/ml IFN-γ. BU.MPT cells were derived from a transgenic mouse bearing a temperature-sensitive mutation (tsA58) of the SV40 large tumor antigen (Tag) under the control of the mouse MHC H-2K^b class I promoter (30, 31). Under permissive conditions, defined as growth at 33°C to 37°C in the presence of IFN-γ, the tsA58 Tag transgene is expressed. Under non-permissive temperatures, defined as growth at 39.5°C in the absence of IFN-γ, expression of the tsA58 Tag transgene is inhibited (by >95%) and BU.MPT cells behave like primary cultures of

mouse kidney PTECs. Prior to all experiments, BU.MPT cells were serum-starved and cultured under non-permissive conditions for 24 h. DO11.10 (DO) cells, a T cell hybridoma line, were grown in RPMI 1640 medium supplemented with 10% (v/v) heat-inactivated FBS, 100 U/ml penicillin/streptomycin, and 50 μ M 2-mercaptoethanol.

Preparation of Apoptotic and Necrotic Cell Targets—Apoptosis of BU.MPT cells was induced by incubating cells in FBS-free medium containing the non-selective protein kinase inhibitor staurosporine (1 μ g/ml, 3 h). Apoptosis of DO cells was induced by incubating cells in FBS-containing medium containing the macromolecular synthesis inhibitor actinomycin D (200 ng/ml, overnight). After induction of apoptosis, the remaining adherent cells were detached by addition of 5 mM EDTA and pooled with floating cells, followed by 3 washes and resuspension in fresh FBS-free medium before use in experiments. For induction of necrosis, cells were first detached with 5 mM EDTA and suspended in the appropriate FBS-free medium. Necrosis was then induced by heating cells to 70°C for 45 min, followed by incubation at 37°C for 2 h. Apoptotic targets were added to responder cells either directly or after fixation for 30 min with 0.4% (v/v) paraformaldehyde in PBS, with similar results. Necrotic targets were always added directly without fixation.

Induction of apoptosis or necrosis was confirmed by flow cytometry. Early apoptotic cells (intact cell membranes) were defined as PI-negative cells with annexin V staining and decreased cell size. Necrotic cells were defined as PI-positive cells of normal or increased cell size. Late apoptotic cells (non-intact cell membranes) were defined as PI-positive cells with annexin V staining and decreased cell size. Loss of membrane integrity by necrotic cells was confirmed by Trypan blue staining. By these criteria, apoptotic target preparations contained ~85% early apoptotic and ~15% late apoptotic cells. Necrotic target preparations contained ~95% necrotic cells. In all preparations, viable cells, defined as PI-negative cells of normal size without annexin V staining, comprised <5% of the total cell population.

Retroviral Transfection with Akt Constructs—BU.MPT cells were infected with retroviral

vectors containing either GFP alone (pBabe-GFP) or GFP plus a constitutively active (myristoylated) Akt construct (pBabe-GFP-myrAkt), both of which were kind gifts of Dr. Nissim Hay (University of Illinois at Chicago, Chicago, IL). Retroviruses were generated by transient transfection of the retroviral vectors into Phoenix ecotropic packaging cell lines, followed by harvesting of the retrovirus-containing culture medium. Myristoylation of Akt leads to its localization at the cell membrane where Akt can be activated via phosphorylation at Thr³⁰⁸ by the upstream kinase 3-phosphoinositide-dependent protein kinase 1 (PDK1). All downstream signaling events, both cytoplasmic and nuclear, dependent on phosphorylation of Akt at Thr³⁰⁸ are replicated by this constitutively active Akt construct (32, 33). Retroviral infection of BU.MPT cells was performed in the presence of 8 μ g/ml polybrene for 24 h. The pBabe-eGFP and pBabe-eGFP-mAkt retroviral vectors, as well as protocols using them, have been previously described (32, 33).

shRNA—BU.MPT cells were transduced with control scrambled or specific anti- β 1-AMPK shRNA constructs cloned into the pGIPZ™ lentiviral vector using the Trans-Lentiviral shRNA Packaging Kit (GE Healthcare Dharmacon Inc, Lafayette, CO). Specific anti- β 1-AMPK shRNA (TGATGTACAAGTTTCAATA) targeted the β 1 isoform of AMPK; control scrambled shRNA (ATCTCGCTTGGGCGAGAGT) was non-silencing. The pGIPZ™ lentiviral vector contains a puromycin resistance gene used to select successfully transduced cells.

Transduction of BU.MPT cells and passaging of transduced cells were performed under permissive conditions (37°C in the presence of IFN- γ). BU.MPT cells were seeded into 24-well tissue culture plates at a density of 5×10^4 cells/well. The following day, 250 μ l of culture medium, containing polybrene (8 μ g/ml) and 1.8×10^7 transduction units of lentiviral particles, was added to each well, according to manufacturer's instructions. After incubation for 6 h, 1 ml of culture medium was added per well, and cells were incubated for an additional 72 h. Cells were then passed into 60 mm dishes containing 5 ml culture medium plus puromycin (1 μ g/ml), in order to select BU.MPT cells successfully transduced with lentiviral constructs.

To confirm knock-down of β 1-AMPK, cells surviving 12 d of puromycin selection were subjected to immunoblotting. As compared to BU.MPT cells transduced with control shRNA, β 1-AMPK expression was reduced by ~75% in cells containing specific shRNA (see Fig. 5a). The β 2-AMPK isoform, not knocked down by β 1-AMPK shRNA, constituted <20% of total AMPK in control- and non-transduced BU.MPT cells. Stably transduced BU.MPT cells were maintained in the presence of puromycin (1 μ g/ml). Prior to all experiments, cells were cultured for 24 h under non-permissive conditions in the absence of puromycin.

Western Blot Analysis—After stimulation of BU.MPT responder cells with apoptotic or necrotic targets, in the presence or absence of EGF (10 nM) (EMD Calbiochem, San Diego, CA), responders were washed 3 times with ice-cold PBS, and then lysed in ice-cold cell lysis buffer (TBS containing 10 mM sodium pyrophosphate, 0.5% w/v deoxycholate, 0.1% w/v SDS, 10% glycerol, 25 mM sodium fluoride, 10% Triton X-100, 1 mM DTT, 1 mM PMSF, 10 mM sodium orthovanadate with added Roche Complete[®] Mini EDTA-free anti-protease mixture tablet). Lysates were sonicated on ice with 10 pulses of 20 Hz, then centrifuged at $20,000 \times g$ for 10 min at 4°C. Supernatants were stored at -70°C.

Protein concentrations of sample for gel electrophoresis were determined by the bicinchoninic acid protein assay (Pierce; Rockford, IL). Samples were then boiled in 6 \times reducing sample buffer for 5 min at 95°C, and 20 μ g per sample were loaded onto 4-15% Mini-PROTEAN[®] TGX precast gels (BioRad; Hercules, CA), electrophoresed at 120 V at constant voltage, and wet transferred on Genie[®] blotter (Idea Scientific, Minneapolis, MN) at 12 V constant voltage to Immobilon-P (0.45 μ m) PVDF membranes (Millipore; Billerica, MA). Membranes were blocked with 5% w/v dry milk in TBS plus 0.1% (v/v) Tween-20, before probing with one of the primary antibodies described above. Following incubation with secondary antibody, immunoreactive bands were visualized by the luminol reaction (GE Healthcare). Equivalent loading of protein samples was monitored by staining with Ponceau S (0.25% w/v) in 0.1% v/v acetic acid for 5 min and/or detection of GAPDH or β -actin.

Flow Cytometric Analysis of Cell Growth—Cell growth was assessed by a modification of previously described methods (27). In brief, BU.MPT responder cells were exposed to apoptotic or necrotic targets for the indicated times, then rinsed twice with PBS. After overnight culture, cells were stained with DAPI (1 μ g/ml) for 30 min at 37°C, harvested by trypsinization, and resuspended in Ca^{2+} - and Mg^{2+} -free PBS containing 2 mM EDTA and 10% (v/v) heat-inactivated FBS. Single-cell suspensions were run on either a BD LSRFortessa flow cytometer with BD FACSDiva[™] acquisition software (BD Biosciences, Franklin Lakes, NJ) or a CyAn[™] ADP flow cytometer with Summit[™] acquisition software (Beckman Coulter, Inc., Fullerton, CA). Cells were gated to exclude cellular aggregates. Gated cells were assessed for DNA content, and the relative size of cells in G1 phase of the cell cycle was determined by measuring forward scatter. Unstained cells, both responders and targets, were used to compensate for spectral spillover. Analysis was performed on either fixed (2% paraformaldehyde for 20 min) or live unfixed responder cells, with similar results.

Measurement of Intracellular AMP, ADP, and ATP—Intracellular content of AMP, ADP, and ATP was measured by modification of previously described methods (34, 35). In brief, after rinsing with ice-cold saline (phosphate-free), cells were scraped and centrifuged at $5000 \times g$ for 4 min at 4°C. After addition of 300 μ l of acidic acetonitrile solvent (80:20 v/v acetonitrile in HPLC water containing 0.1 M formic acid), the pellet was incubated on ice for 15 min, and then centrifuged at $20,000 \times g$ for 5 min at 4°C. The supernatant was separated, and an additional 200 μ l of acidic acetonitrile solvent was added to the pellet, followed again by centrifugation at $20,000 \times g$ for 5 min at 4°C. This step was repeated a third time, and the supernatants were combined to a final volume of 700 μ l.

Extracts were then analyzed with the 5500 QTRAP liquid chromatography-tandem mass spectrometry (LC/MS/MS) system (AB Sciex, Foster City, CA) with a 1200 series HPLC system (Agilent Technologies, Santa Clara, CA) including a degasser, an autosampler, and a binary pump. The LC separation was performed on a Phenomenex 5u C18(2) column (4.6 x 250 mm, 5

μm) with mobile phase A (25 mM ammonia acetate in water) and mobile phase B (methanol). The flow rate was 0.55 mL/min. The linear gradient was as follows: 0-1 min, 95% phase A; 6-10.5 min, 1% phase A; 10.6-19 min, 95% phase A. The autosampler was set at 5°C. The injection volume was 10 μL. Mass spectra were acquired under negative electrospray ionization with an ion spray voltage of -4500 V. The source temperature was 500°C. The values for the curtain gas, ion source gas 1, and ion source gas 2 were 35, 65, and 55 pounds per square inch, respectively. Multiple reaction monitoring (MRM) was used for quantitation: ATP mass-to-charge ratio (m/z) 506.1 → m/z 79.0; ADP m/z 426.1 → m/z 79.0; and AMP m/z 346.1 → m/z 79.0. The internal standard 2-chloro-ATP was monitored at m/z 540.0 → m/z 79.0.

Statistics—Data are expressed as mean ± SEM of the averaged values obtained from each experiment. Statistical significance was determined by a two-tailed Student's t-test.

RESULTS

Apoptotic Targets Inhibit the Growth of Live BU.MPT Responder Cells—We have shown previously that receptor-mediated recognition of apoptotic targets induces the apoptotic death and inhibits the proliferation of viable BU.MPT epithelial cell responder cells (8, 9). Both activities lead to a decrease in the magnitude of the responder cell population, thereby reducing the population's metabolic demand. If the surge in the number of apoptotic targets is the consequence of a diminished metabolic supply, as for example from ischemia, then these two target-induced activities would tend to restore the balance between supply and demand. As cells can also reduce their metabolic demand by decreasing protein synthesis and other energy-consuming anabolic pathways, we determined the effect of apoptotic targets on cell size during G1 phase of the cell cycle, a measure of cell mass or growth (26-29).

BU.MPT responders were exposed to apoptotic or necrotic targets for 2 h (Fig. 1). After 24 h, the relative size of responders in G1 phase of the cell cycle was assessed by flow cytometric comparison of forward scatter (27). Apoptotic

targets significantly decreased the relative size of BU.MPT responders to $64.3 \pm 7.3\%$ of that of untreated responders ($p < 0.02$) (Fig. 1B). In contrast, necrotic targets lacked a significant effect on the relative size of BU.MPT responders ($90.5 \pm 5.6\%$; $p =$ not significant). Although the primary source of apoptotic targets in these studies was murine DO T-cells induced to undergo apoptosis by treatment with actinomycin D, similar results were obtained with BU.MPT targets induced to undergo apoptosis by treatment with staurosporine (data not shown).

The major controller of cell growth is the mTORC1-regulated ribosomal kinase, p70S6K (27-29). We therefore determined the effect of apoptotic targets on both basal and EGF-induced p70S6K phosphorylation and activity (Fig. 2A). Exposure of quiescent BU.MPT responders to apoptotic targets for 15 min strongly inhibited basal phosphorylation of p70S6K. Similarly, prior exposure to apoptotic targets strongly inhibited EGF-induced phosphorylation of p70S6K. In both cases, inhibition of p70S6K occurred in a dose-dependent manner. Inhibition of p70S6K phosphorylation correlated with inhibition of p70S6K activity, as detected by parallel inhibition of phosphorylation of the ribosomal protein S6, a downstream target of p70S6K. Remarkably, inhibition occurred at ratios below one apoptotic target per BU.MPT responder cell. Inhibition was evident at a target to responder cell ratio as low as 1:32, particularly in the absence of EGF, and was virtually complete at ratios of 1:4 or 1:2. These effects were specific to apoptotic targets, since exposure to necrotic targets had a minimal to undetectable effect on the phosphorylation status of p70S6K and S6, whether added alone or in the presence of EGF (Fig. 2B).

Apoptotic Targets Activate AMPK, a Major Upstream Inhibitor of p70S6K—Control of cell growth and p70S6K occurs primarily through mTORC1, a multimolecular serine/threonine kinase complex (26-29). mTORC1 acts as a sensor of the adequacy of factors and conditions necessary for cell growth and proliferation. Information is derived by continuous monitoring within four major areas: (1) the sufficiency of cellular energy stores; (2) the availability of growth factors such as EGF; (3) the adequacy of nutrients such as glucose and amino acids; and (4) the presence and extent of cell damage. Input

from these multiple sources can either raise or lower the overall activity of mTORC1, thereby enabling each cell to adjust its metabolic activity to a level appropriate for the prevailing environment (26-29).

The sensing of energy status is dependent primarily on the activity of the intracellular kinase AMPK, a heterotrimeric protein whose activation correlates with phosphorylation of its catalytic α -subunit at Thr¹⁷² (23-25). The β - and γ -subunits are both regulatory. When activated, AMPK inhibits mTORC1 in several ways, both direct and indirect (23-25). As a test of our hypothesis that apoptotic targets act as an extracellular stress, mimicking the effects of intracellular depletion of energy stores, we determined the degree of AMPK phosphorylation following exposure of BU.MPT responders to apoptotic targets (Fig. 3A). Consistent with their unstressed state, quiescent BU.MPT responders displayed a low basal level of AMPK phosphorylation. Exposure to apoptotic targets, either alone or in the presence of EGF, induced a dose-dependent increase in the phosphorylation of AMPK. As with inhibition of phosphorylation of p70S6K, increased phosphorylation of AMPK was observed at a target to responder ratio as low as 1:32. Exposure to necrotic targets produced no detectable change in phosphorylation of AMPK.

A second major input to mTORC1 derives from the survival kinase Akt, which is activated by growth factors like EGF. We have shown previously that apoptotic targets inhibit the phosphorylation of Akt at Ser⁴⁷³ (8, 9). Phosphorylation at this site is performed by mTORC2, a second mTOR-containing multimolecular kinase complex (28). Since an uncertain relationship exists between the activities of mTORC1 and mTORC2, we also examined phosphorylation of Akt at Thr³⁰⁸, an event which occurs upstream of mTORC1. Phosphorylation of Akt at Thr³⁰⁸ is mediated by PDK1 and increases the activity of mTORC1 (32, 33).

Exposure to apoptotic targets induced a dose-dependent decrease in phosphorylation of Akt at both Thr³⁰⁸ and Ser⁴⁷³ (Fig 3B). Basal phosphorylation at these two sites was low, so that inhibition was most evident in the presence of EGF. Inhibition of phosphorylation of Akt correlated with inhibition of its activity, as detected by parallel inhibition of phosphorylation

of the kinase GSK3 α/β (downstream of the Thr³⁰⁸ site) and the transcription factors FoxO1 and Fox3a (downstream of the Ser⁴⁷³ site). Necrotic targets had a greatly diminished effect as compared to apoptotic targets, and, if anything, increased slightly the phosphorylation and activity of Akt (Fig. 3B).

Taken together, these data indicate that exposure to apoptotic targets provokes two signaling events known to lower the activity of mTORC1, namely, activation of AMPK and inhibition of Akt. Via subsequent decreased mTORC1-mediated phosphorylation of p70S6K, these two signaling events likely play an important role in the observed inhibition of BU.MPT responder cell growth following exposure to apoptotic targets.

Inhibition of AMPK, Either Pharmacologically or Molecularly, Prevents Apoptotic Target-Induced Inhibition of Cell Growth—To establish a mechanistic link between activation of AMPK and inhibition of cell growth following exposure to apoptotic targets, we determined the effect of inhibition of AMPK, either pharmacologically via compound C (CC) (Fig. 4) or molecularly via shRNA (Fig. 5). CC, which inhibits AMPK by reversible competition with AMP for binding to AMPK, has been used to explore the role of AMPK in multiple tissues and cells, including BU.MPT cells (36-38). BU.MPT responders were pretreated with varying concentrations of CC for 2 h prior to exposure to apoptotic targets. As shown in Fig. 4A, pharmacologic inhibition of AMPK restored phosphorylation of both p70S6K and S6 to levels observed in cells not exposed to apoptotic targets. Notably, in contrast to its dose-dependent inhibition of the effect of apoptotic targets, CC did not modulate the response to necrotic targets.

Several points merit emphasis. First, in support of the specificity of CC for AMPK, pretreatment with CC had a minimal effect on apoptotic target-induced inhibition of phosphorylation of GSK3 α/β , a downstream target of Akt. Second, despite inhibition of the downstream effects of AMPK, CC had no detectable effect on phosphorylation of AMPK at Thr¹⁷². This differs from our previous results, in which CC inhibited phosphorylation of AMPK in response to ATP depletion (38), perhaps indicating a non-canonical activation of AMPK by apoptotic

targets (see below). Finally, total levels of AMPK were unaffected by CC and/or apoptotic targets. BU.MPT cells express both β -isoforms of AMPK (β 1- and β 2-AMPK); of these, β 1-AMPK is the more abundant (>80% by densitometry).

Consistent with its restoration of p70S6K phosphorylation and activity, CC (10 μ M) also prevented inhibition of cell growth (Fig 4, B and C). In the absence of CC, apoptotic targets significantly decreased the relative size of BU.MPT responders to $77.2 \pm 3.6\%$ of that of untreated responders ($p < 0.05$) (Fig. 4C). In contrast, in the presence of CC, the relative size of BU.MPT responders was $109.9\% \pm 2.2\%$ of that of responders not treated with CC or exposed to apoptotic targets ($p < 0.02$, CC *versus* no CC). CC also increased the relative size of responders exposed to necrotic or no targets. This suggests that under the conditions of our studies AMPK may be exerting a tonic basal inhibition of cell growth.

As the use of pharmacological inhibitors is subject to problems of specificity, we sought a second independent approach to inhibit AMPK. To this end, we used shRNA to knock down expression of the regulatory β -subunit of AMPK (Fig. 5). We targeted the β 1 isoform of AMPK, as its expression greatly exceeds that of the β 2 isoform in BU.MPT cells (Fig. 4A). The targeted shRNA reduced total AMPK by ~75% compared with control shRNA (Fig. 5A).

Overall, molecular inhibition of AMPK replicated the results seen with pharmacological inhibition (Fig. 5). In accord with its knock-down of total AMPK, β 1-AMPK shRNA reduced the degree of upregulation of Thr¹⁷² phosphorylation of AMPK in response to apoptotic targets. Knock-down of AMPK restored phosphorylation of p70S6K and S6 in apoptotic target-treated responders to levels equal to or greater than those observed in untreated responder cells. As with CC, inhibition of the phosphorylation of GSK3 α / β was unaffected by knock-down. Importantly, the responses of BU.MPT cells transduced with control scrambled shRNA were indistinguishable from those of untransduced BU.MPT cells.

Knock-down of AMPK also reduced the ability of apoptotic targets to inhibit cell growth (Fig 5, B and C). For BU.MPT cells transduced with control shRNA, exposure to apoptotic targets

significantly decreased the relative size of responders to $66.1 \pm 5.9\%$ of that of unexposed responders ($p < 0.01$) (Fig. 4C). In contrast, for BU.MPT cells transduced with β 1-AMPK shRNA, exposure to apoptotic targets reduced the relative size of responders to only $90.0 \pm 3.5\%$ of that of untreated responders ($p < 0.03$, presence *versus* absence of apoptotic targets). The reduction of cell size by responders expressing β 1-AMPK shRNA was significantly less than that by responders expressing scrambled shRNA ($p < 0.02$, β 1-AMPK *versus* scrambled shRNA, presence of apoptotic targets).

Inhibition of Akt Also Contributes to Inhibition of Cell Growth by Apoptotic Targets—Inhibition of the phosphorylation and activity of Akt by apoptotic targets is most evident in the presence of growth factors like EGF (Fig. 3B). Since the availability of growth factors represents a second major input to mTORC1, we next determined the contribution of inhibition of Akt to inhibition of cell growth following exposure to apoptotic targets. To do so, we stably infected BU.MPT cells with a myristoylated Akt (myrAkt)-GFP retroviral construct (32, 33). Myristoylation of Akt leads to its surface membrane localization and constitutive activity (32, 33). BU.MPT cells expressing myrAkt, hereafter denoted as BU.MPT-myrAkt-GFP, were detected by co-expressed GFP. BU.MPT control cells, infected with a retroviral construct containing GFP alone, are denoted as BU.MPT-GFP.

BU.MPT-myrAkt-GFP responders demonstrated increased phosphorylation at both the PDK1 site (Thr³⁰⁸) and the mTORC2 site (Ser⁴⁷³) (Fig. 6A). In accord with the constitutive activation of Akt in BU.MPT-myrAkt-GFP cells, phosphorylation at Thr³⁰⁸ and Ser⁴⁷³ was not affected by exposure to apoptotic targets or pretreatment with CC. Control BU.MPT-GFP cells showed phosphorylation of Akt only at Ser⁴⁷³, which was inhibited by exposure to apoptotic targets. Inhibition was reversed by CC, suggesting that mTORC2 may lie downstream of AMPK. Alternatively, this may represent an off-target effect of CC.

Inhibition of the phosphorylation of p70S6K and S6 did not occur in BU.MPT-myrAkt-GFP responders, despite potent phosphorylation of AMPK following exposure to apoptotic targets

(Fig. 6B). This lack of inhibition resembles that observed with inhibition of AMPK (Figs. 4 and 5). As expected with constitutive activation of Akt, apoptotic targets did not inhibit Akt-mediated phosphorylation of GSK3 α/β in BU.MPT-myrAkt-GFP responders.

Notably, despite restoration of the phosphorylation of p70S6K and S6 in BU.MPT-myrAkt-GFP responders, inhibition of cell growth was still observed (Fig. 6, C and D). Relative size following exposure to apoptotic targets was reduced to $76.0 \pm 3.1\%$ in BU.MPT-GFP responders ($p < 0.001$) as opposed to $82.8 \pm 1.7\%$ in BU.MPT-myrAkt-GFP responders ($p < 0.05$). Although the reduction of cell size occurring in BU.MPT-myrAkt-GFP responders was significantly less than that in BU.MPT-myrAkt-GFP responders ($p < 0.05$), the degree of improvement was still less than that observed with inhibition of AMPK, either pharmacologically by CC ($p < 0.001$) or molecularly by shRNA ($p < 0.05$). Thus, of the two signaling events contributing to growth inhibition – namely, activation of AMPK and inhibition of Akt – prevention of AMPK activation largely abrogated cell growth inhibition (Figs. 4C and 5C), whereas prevention of Akt inhibition only partially abrogated cell growth inhibition (Fig. 6C). Together, these data suggest that AMPK activation plays the greater role in apoptotic target-mediated inhibition of cell growth.

Apoptotic Targets Activate AMPK Independently of Changes in Intracellular Energy Stores—AMPK is a heterotrimeric kinase activated by decreasing concentrations of ATP and increasing concentrations of AMP and ADP (23–25). Activation of AMPK depends on phosphorylation of its catalytic subunit at Thr¹⁷². Binding of either AMP or ADP promotes phosphorylation of AMPK at this site. In addition, binding of AMP, but not ADP, can directly activate AMPK. AMP sustains AMPK activity by inhibiting its dephosphorylation, whereas ATP promotes dephosphorylation. Thus, both ADP to ATP and AMP to ATP ratios contribute to AMPK regulation.

To determine whether apoptotic targets activate AMPK by inducing changes in intracellular energy stores, we measured intracellular concentrations of AMP, ADP, and ATP by LC/MS/MS in BU.MPT responders

following exposure to apoptotic targets (Fig. 7). The calculated quantity of energy charge represents the fraction of adenylate-bound high energy phosphate bonds present as compared to the maximum possible, and is defined by the formula.

$$\frac{[ATP] + \frac{1}{2}[ADP]}{[ATP] + [ADP] + [AMP]}$$

This formula yields a value between 0 (100% AMP) and 1 (100% ATP).

Exposure to apoptotic targets for 2 h produced no detectable change in either ADP to ATP ratio, AMP to ATP ratio, or energy charge at either 0.5 h or 18 h following exposure ($p > 0.8$). The first time corresponds to that at which we performed all immunoblots. The absence of a change in intracellular energy stores at a time when AMPK is strongly phosphorylated (see Figures 3, 4A, 5A, and 6B) provides powerful evidence that exposure to apoptotic targets induces activation of AMPK via an energy-independent pathway (23–25). As further support for this idea, we also assessed intracellular energy stores at 18 h, since this later time corresponds to that at which we performed all flow cytometric analyses of growth inhibition. Again, there was no detectable change in intracellular levels of AMP, ADP, or ATP.

Inhibition of Cell Growth by Apoptotic Targets Depends on Cell-Cell Interaction but Is Independent of Phagocytosis—BU.MPT responders were grown in a Transwell® permeable support system and separated from apoptotic targets by a 0.4 μ M polycarbonate membrane. Prevention of physical interaction between BU.MPT responders and apoptotic targets abolished the ability of apoptotic targets to inhibit cell growth (Fig. 8A). Necrotic targets had no effect on relative cell volume, irrespective of the presence or absence of the Transwell® permeable support system (data not shown).

To test the role of phagocytosis, we used the cytoskeletal inhibitor cytochalasin D to prevent phagocytosis. Inhibition of cell growth in response to apoptotic targets occurred in the absence of phagocytosis (Fig. 8B). We obtained comparable data with two concentrations of cytochalasin D, both of which inhibit m ϕ and BU.MPT phagocytosis by $\geq 90\%$ (8, 9). Necrotic targets had no effect on relative cell volume, irrespective of the presence or absence of

cytochalasin D (data not shown). Taken together, our results show that apoptotic target-mediated inhibition of BU.MPT growth requires direct physical interaction between targets and responder cells but is independent of phagocytosis.

DISCUSSION

We show here that exposure of live kidney PTECs to apoptotic target cells inhibits PTEC cell growth, as manifested by a decreased size of cells in G1 phase of the cell cycle. Apoptotic targets inhibit cell growth by modulating the activity of at least two intracellular signaling pathways, both of which converge on mTORC1. The first pathway results from inhibition of Akt, a survival kinase whose activation raises the activity of mTORC1 (28, 39-43). By inhibiting Akt, apoptotic targets lower mTORC1 activity, and therefore the activity of the ribosomal kinase p70S6K, a key regulator of cell growth and an immediate downstream target of mTORC1 (26-29). The second pathway influenced by apoptotic targets results from activation of AMPK, a critical sensor of intracellular energy stores (23-25, 28). Activation of AMPK by apoptotic targets provides a second inhibitory input to mTORC1. Remarkably, activation of AMPK by apoptotic targets occurs in an energy-independent manner, without detectable changes in intracellular levels of ATP, ADP, or AMP. These events are all specific to apoptotic targets. Exposure to necrotic targets produced no detectable effect on cell growth or AMPK activity, and, if anything, weakly stimulated Akt. Consistent with our previous observations that kidney PTECs recognize apoptotic *versus* necrotic targets via distinct receptors (8, 9), inhibition of PTEC cell growth by apoptotic targets requires direct physical interaction between targets and PTEC responders. As in our previous studies (8, 9), inhibition of cell growth was independent of phagocytosis.

Of the two signaling events leading to apoptotic target-mediated inhibition of cell growth – namely, activation of AMPK and inhibition of Akt – AMPK activation appears to be the more potent. The dominance of AMPK activation as a mediator of growth inhibition by apoptotic targets is seen by comparison of Figs. 4C and 5C with Fig. 6D. Reversal of AMPK activation almost

completely abrogated cell growth inhibition by apoptotic cells, whereas reversal of Akt inhibition only partially abrogated cell growth inhibition. Thus, pharmacologic inhibition of AMPK with CC increased relative cell size from $77.2 \pm 3.6\%$ to $109.9\% \pm 2.2\%$ ($p < 0.02$), and, similarly, molecular inhibition of AMPK increased relative cell size from $66.1 \pm 5.9\%$ to $90.0\% \pm 3.5\%$ ($p < 0.02$). In marked contrast, constitutive activation of Akt only increased relative size from $76.0 \pm 3.1\%$ to $82.8 \pm 1.7\%$. The degree of improvement with activation of Akt was significantly less than that observed with inhibition of AMPK, either pharmacologically by CC ($p < 0.001$) or molecularly by shRNA ($p < 0.05$). These data indicate that activation of AMPK in response to apoptotic targets exerts a greater growth inhibitory effect than does inhibition of Akt.

A potential explanation may lie in the mechanisms by which Akt and AMPK modulate mTORC1 activity. Whereas Akt raises the activity of mTORC1, AMPK lowers its activity (28). In the case of Akt, mTORC1 activation involves a release of inhibition through phosphorylation of two negative regulators of mTORC1. The first target of Akt is the tuberous sclerosis complex (TSC) component tuberlin (TSC2), an upstream inhibitor of mTORC1 (39-41). The second target of Akt is PRAS40, a negative regulator within the mTORC1 complex. Phosphorylation of PRAS40 by Akt causes its dissociation from mTORC1 (42, 43). Relief of inhibition from these two sources, the first upstream of mTORC1 and the second within the mTORC1 complex, leads to activation of mTORC1. Like Akt, AMPK targets both TSC2 and a protein within the mTORC1 complex, but phosphorylation by AMPK has opposite effects to those of Akt. Thus, phosphorylation of TSC2 by AMPK leads to the activation of this upstream inhibitor of mTORC1 (44, 45). The second AMPK target is Raptor, a scaffold protein necessary for the assembly of mTORC1 as well as for interaction of mTORC1 with its various substrates and regulators. Phosphorylation of Raptor by AMPK leads to Raptor's sequestration by 14-3-3 proteins, rendering Raptor incapable of fulfilling its role as a scaffolding molecule (46). Since Akt and AMPK have overlapping targets, the greater potency of AMPK in inhibiting cell growth may reflect the dominance of inhibitory over stimulatory signals. For example,

dissociation of the negative regulator PRAS40 from mTORC1 may be of lesser relevance if Raptor, the scaffold upon which mTORC1 assembles, is sequestered and unavailable. Alternatively, the seemingly greater potency of AMPK activation over Akt inhibition may reflect off-target effects of CC and/or differences in the penetrance and effectiveness between the myrAkt and β 1-AMPK shRNA constructs.

The lack of a detectable change in ADP to ATP ratio, AMP to ATP ratio, or energy charge following exposure to apoptotic targets implies that activation of AMPK occurs in an energy-independent manner. Thus, despite strong phosphorylation and activation of AMPK at 0.5 h following exposure to apoptotic targets (see Figs. 3, 4A, 5A, and 6B), intracellular stores of energy are unchanged at this time (see Fig. 7). Phosphorylation of the catalytic α -subunit of AMPK at Thr¹⁷² increases AMPK activity by more than 100-fold (23-25). The major upstream kinase responsible for phosphorylating AMPK in response to energy stress is liver kinase B1 (LKB1) (23-25, 47). Phosphorylation of AMPK by LKB1 is enhanced by binding of ADP and AMP to the γ -subunit of AMPK. Binding of ADP and AMP also inhibits dephosphorylation of AMPK (23-25). AMP has an additional effect not shared by ADP. Allosteric changes induced by binding of AMP, but not ADP, further increase AMPK activity by as much as 10-fold (23). However, activation of AMPK by LKB1 has been described only under circumstances of energy stress. Therefore, unless exposure to apoptotic targets induces signaling events that permit LKB1 to phosphorylate AMPK in the absence of a change in intracellular energy stores, LKB1 is unlikely to mediate AMPK activation in our system.

A second kinase capable of phosphorylating AMPK at Thr¹⁷² of its α -subunit is Ca^{2+} /calmodulin-activated protein kinase kinase β (CaMKK β , also known as CAMKK2) (23, 48). In LKB1-deficient cells, CaMKK β phosphorylates and activates the α -subunit of AMPK at Thr¹⁷² in response to an increase of intracellular Ca^{2+} (49). Interestingly, purified CaMKK β forms a stable multiprotein complex *in vitro* with the α - and β -subunits of AMPK. Since the AMP- and ADP-binding γ -subunit of AMPK is absent,

phosphorylation and activation of AMPK within this complex is regulated by Ca^{2+} , but not AMP or ADP (50, 51). The *in vivo* significance of this observation remains uncertain (52). Besides increased intracellular Ca^{2+} , several other signaling molecules, such as protein kinase A (PKA), are known to modulate the activity of CaMKK β (53).

In addition to LKB1 and CaMKK β , a number of other proteins, second messengers, and intracellular stresses have been reported to modulate the activity of AMPK. Although their mechanisms of activation remain unclear, these include second messengers like cAMP (53, 54), proteins and kinases such as p53 (55), PKA (54), and ataxia telangiectasia mutated (ATM) (56), and a variety of intracellular stresses such as oxidative (23, 28, 56, 57), and genotoxic (23, 28, 55). Future studies will address whether any of these molecules participate in the activation of AMPK by apoptotic targets, or whether apoptotic targets activate AMPK via an as yet unrecognized and novel pathway.

Regardless of the pathway by which apoptotic targets activate AMPK, it appears that PTECs respond to the extracellular presence of apoptotic targets as if subjected to a metabolic or other stress. Together with previous work from our and other laboratories (3-9, 16-18), our results suggest that the network of signaling responses to dead targets, as observed in viable responder cells of multiple lineages, represents a critical and ubiquitous dimension of tissue homeostasis. We hypothesize that, throughout the body, local alterations in the mode and extent of cell death alert viable resident cells in the vicinity to environmental change or stress (9, 22). A local increase in the number of dead or dying cells may be triggered by diverse stresses such as ischemia, infection, aging, or acute injury. Viable resident cells can then extract information about the nature of the stress, and the possibility for adaptation, via their interaction with adjacent dead or dying cells. Responding cells gauge the severity of the environmental disturbance not simply from the number of dead cells, but also from the mode of death (apoptotic *versus* necrotic), pattern of distribution of dead cells, and timing of their appearance. For example, in the case of necrotic targets, the disturbance is likely to be sudden and catastrophic, whereas, in the case of apoptotic targets, it may be more gradual and potentially

adaptable. Such considerations may underlie the observation that, in general, the responses elicited by apoptotic *versus* necrotic targets are oppositely directed (3-6, 8, 9, 22). For example, we have previously shown that apoptotic targets inhibit the proliferation and survival of PTECs, while necrotic targets promote these activities (8, 9). In the present study, we show that apoptotic targets activate AMPK and inhibit cell growth, while the effect of necrotic targets is minimal or neutral.

It is important to emphasize that the cellular response to dead targets is varied, robust, and complex. This breadth of response permits cells and organs to tailor their behavior to function and need. Thus, within an organ, the responses of nearby resident cells may vary considerably, depending on their lineage or differentiative stage (6-9, 17-19, 22). Even for responder cells of similar lineage, responses can differ depending on their organ of origin or state of activation (9, 20).

Seen in light of this hypothesis, inhibition of PTEC cell growth following exposure to apoptotic targets may represent one aspect of an overall adaptive strategy, in response to a threatened reduction in metabolic supply. Activation of AMPK initiates a wide range of intracellular events that affect intermediary cell metabolism. The net result is the conservation or augmentation of intracellular energy stores, through increased energy production, decreased energy consumption, and facilitated cellular uptake of nutrients (23, 24). Metabolic demand by PTECs is further decreased following exposure to apoptotic targets by a

reduction in population size, brought about through the combined effects of decreased proliferation and increased cell death (8, 9). Thus, in the case of PTECs, exposure to apoptotic targets produces a stress response, whose ultimate effect is a drastic reduction in metabolic demand, achieved via a decrease not only in the number of live cells but also in the energy expenditure per cell.

In summary, we have shown that exposure to apoptotic targets inhibits the growth of live PTEC responders. At least two signaling events cooperate to produce this inhibition, namely, inhibition of Akt and activation of AMPK. Activation of AMPK occurs without detectable change in intracellular energy stores. These data offer further support to the hypothesis that the recognition of apoptotic targets by live responder cells represents an important source of information for responder cells about their environment. In the case of PTECs, a highly metabolic lineage, apoptotic cells serve as an extracellular stress, mimicking the effects of depletion of intracellular energy stores. By acting as sentinels of environmental change, apoptotic targets permit nearby cells to monitor their environment and adapt to local changes. Adaptation involves the modulation of multiple critical cell activities. These include the proliferation, survival, and, as shown here, growth of responder cells.

CONFLICT OF INTEREST STATEMENT

No author has an actual or perceived conflict of interest with the contents of this article.

AUTHOR CONTRIBUTIONS

JSL developed the central hypothesis of the manuscript and its study design, wrote the article, and was responsible for final approval of the version to be published. VAP, DM, SV, LF, MT, and NL made substantial contributions to acquisition, analysis, and interpretation of data. VAP, DM, SV, AA, JR, and WL contributed to the conception and design of studies. SV, AA, JR, and WL made critical revisions to the manuscript. All authors reviewed the results and approved the final version of the manuscript.

REFERENCES

1. Wallach, D., Kang, T.-B., and Kovalenko, A. (2014) Concepts of tissue injury and cell death in inflammation: a historical perspective. *Nature Rev. Mol. Cell Biol.* **14**, 51–59
2. Hochreiter-Hufford, A., and Ravichandran, K. S. (2013) Clearing the dead: Apoptotic cell sensing, recognition, engulfment, and digestion. *Cold Spring Harb. Perspect. Biol.* **5**, a008748
3. Reddy, S. M., Hsiao, K. H., Abernethy, V. E., Fan, H., Longacre, A., Lieberthal, W., Rauch, J., Koh, J. S., and Levine, J. S. (2002) Phagocytosis of apoptotic cells by macrophages induces novel signaling events leading to cytokine-independent survival and inhibition of proliferation: activation of Akt and inhibition of extracellular signal-regulated kinases 1 and 2. *J. Immunol.* **169**, 702–713
4. Cvetanovic, M., and Ucker, D. S. (2004) Innate immune discrimination of apoptotic cells: repression of proinflammatory macrophage transcription is coupled directly to specific recognition. *J. Immunol.* **172**, 880–889
5. Patel, V. A., Longacre, A., Hsiao, K., Fan, H., Meng, F., Mitchell, J. E., Rauch, J., Ucker, D. S., and Levine, J. S. (2006) Apoptotic cells, at all stages of the death process, trigger characteristic signaling events that are divergent from and dominant over those triggered by necrotic cells: implications for the delayed clearance model of autoimmunity. *J. Biol. Chem.* **281**, 4663–4670
6. Cvetanovic, M., Mitchell, J. E., Patel, V., Avner, B. S., Su, Y., van der Saag, P. T., Witte, P. L., Fiore, S., Levine, J. S., and Ucker, D. S. (2006) Specific recognition of apoptotic cells reveals a ubiquitous and unconventional innate immunity. *J. Biol. Chem.* **281**, 20055–20067
7. Birge, R. B., and Ucker, D. S. (2008) Innate apoptotic immunity: the calming touch of death. *Cell Death Differ.* **15**, 1096–1102
8. Patel, V. A., Lee, D. J., Feng, L., Antoni, A., Lieberthal, W., Schwartz, J. H., Rauch, J., Ucker, D. S., and Levine, J. S. (2010) Recognition of apoptotic cells by epithelial cells: conserved versus tissue-specific signaling responses. *J. Biol. Chem.* **285**, 1829–1840
9. Patel, V. A., Feng, L., Lee, D. J., Massenburg, D., Pattabiraman, G., Antoni, A., Schwartz, J. H., Lieberthal, W., Rauch, J., Ucker, D. S., and Levine, J. S. (2012) Recognition-dependent signaling events in response to apoptotic targets inhibit epithelial cell viability by multiple mechanisms: implications for non-immune tissue homeostasis. *J. Biol. Chem.* **287**, 13761–13777
10. Voll, R. E., Herrmann, M., Roth, E. A., Stach, C., Kalden, J. R., and Girkontaite, I. (1997) Immunosuppressive effects of apoptotic cells. *Nature* **390**, 350–351
11. Fadok, V. A., Bratton, D. L., Konowal, A., Freed, P. W., Westcott, J. Y., and Henson, P. M. (1998) Macrophages that have ingested apoptotic cells in vitro inhibit proinflammatory cytokine production through autocrine/ paracrine mechanisms involving TGF- β , PGE₂, and PAF. *J. Clin. Invest.* **101**, 890–898
12. Lucas, M., Stuart, L. M., Savill, J., and Lacy-Hulbert, A. (2003) Apoptotic cells and innate immune stimuli combine to regulate macrophage cytokine secretion. *J. Immunol.* **171**, 2610–2615
13. Ariel, A., Fredman, G., Sun, Y.-P., Kantarci, A., Van Dyke, T. E., Luster, A. D., and Serhan, C. N. (2006) Apoptotic neutrophils and T cells sequester chemokines during immune response resolution through modulation of CCR5 expression. *Nature Immunol.* **7**, 1209–1216, 2006
14. Schwab, J. M., Chiang, N., Arita, M., and Serhan, C. N. (2007) Resolvin E1 and protectin D1 activate inflammation-resolution programmes. *Nature* **447**, 869–874
15. Rothla, C. V., Ghosh, S., Zuniga, E. I., Oldstone, M. B. A., and Lemke, G. (2007) TAM receptors are pleiotropic inhibitors of the innate immune response. *Cell* **131**, 1124–1136
16. Li, F., Huang, Q., Chen, J., Peng, Y., Roop, D. R., Bedford, J. S., and Li, C.-Y. (2010) Apoptotic cells can activate the "phoenix rising" pathway to promote wound healing and tissue regeneration. *Sci. Signal.* **3**, ra13
17. Peter, C., Wesselborg, S., Hermann, M., and Lauber, K. (2010) Dangerous attraction: phagocyte recruitment and danger signals of apoptotic and necrotic cells. *Apoptosis* **15**, 1007–1028
18. Hess, K. L., Tudor, K.-S. R. S., Johnson, J. D., Osati-Ashtiani, F., Askew, D. S., and Cook-Mills

- J. M. (1997) Human and murine high endothelial venule cells phagocytose apoptotic leukocytes. *Exp. Cell Res.* **236**, 404-411
19. Zerneck, A., Bidzhekov, K., Noels, H., Shagdarsuren, E., Gan, L., Denecke, B., Hristov, M., Köppel, T., Jahantigh, M. N., Lutgens, E., Wang, S., Olson, E. N., Schober, A., and Weber, C. (2009) Delivery of microRNA-126 by apoptotic bodies induces CXCL12-dependent vascular protection. *Sci. Signal.* **2**, ra81
20. Esmann, L., Idel, C., Sarkar, A., Hellberg, L., Behmen, M., Möller, S., van Zandbergen, G., Klinger, M., Köhl, J., Bussmeyer, U., Solbach, W., and Laskay, T. (2010) Phagocytosis of apoptotic cells by neutrophil granulocytes: diminished proinflammatory neutrophil functions in the presence of apoptotic cells. *J. Immunol.* **184**, 391-400
21. Obeid, M., Tesniere, A., Ghiringhelli, F., Fimia, G. M., Apetoh, L., Perfettini, J.-L., Castedo, M., Mignot, G., Panaretakis, T., Casares, N., Métivier, D., Larochette, N., van Endert, P., Ciccosanti, F., Piacentini, M., Zitvogel, L., and Kroemer, G. (2007) Calreticulin exposure dictates the immunogenicity of cancer cell death. *Nature Med.* **13**, 54-61
22. Patel, V. A., Lee, D. J., Longacre-Antoni, A., Feng, L., Lieberthal, W., Rauch, J., Ucker, D. S., and Levine, J. S. (2009) Apoptotic and necrotic cells as sentinels of local tissue stress and inflammation: response pathways initiated in nearby viable cells. *Autoimmunity* **42**, 317-321
23. Hardie, D. G., Ross, F. A., and Hawley, S. A. (2012) AMPK: a nutrient and energy sensor that maintains energy homeostasis. *Nat. Rev. Mol. Cell Biol.* **13**, 251-262
24. Steinberg, G. R., and Kemp, B. E. (2009) AMPK in health and disease. *Physiol. Rev.* **89**, 1025-1078
25. Oakhill, J. S., Steel, R., Chen, Z.-P., Scott, J. W., Ling, N., Tam, S., and Kemp, B. E. (2011) AMPK is a direct adenylate charge-regulated protein kinase. *Science* **332**, 1433-1435.
26. Ma, X. M., and Blenis, J. (2009) Molecular mechanisms of mTOR-mediated translational control. *Nat. Rev. Mol. Cell Biol.* **10**, 307-318
27. Dowling, R. J., Topisirovic, I., Alain, T., Bidinosti, M., Fonseca, B. D., Petroulakis, E., Wang, X., Larsson, O., Selvaraj, A., Liu, Y., Kozma, S. C., Thomas, G., and Sonenberg, N. (2010) mTORC1-mediated cell proliferation, but not cell growth, controlled by the 4E-BPs. *Science* **328**, 1172-1176
28. Lieberthal, W., and Levine, J. S. (2012) Mammalian target of rapamycin and the kidney. I: The signaling pathway. *Am. J. Physiol. Renal Physiol.* **303**, F1-F10
29. Magnuson, B., Ekim, B., and Fingar, D. C. (2012) Regulation and function of ribosomal protein S6 kinase (S6K) within mTOR signalling networks. *Biochem. J.* **441**, 1-21
30. Sinha, D., Wang, Z., Ruchalski, K. L., Levine, J. S., Krishnan, S., Lieberthal, W., Schwartz, J. H., and Borkan, S. C. (2005) Lithium activates the Wnt and phosphatidylinositol 3-kinase Akt signaling pathways to promote cell survival in the absence of soluble survival factors. *Am. J. Physiol. Renal Physiol.* **288**, F703-F713
31. Jat, P. S., Noble, M. D., Ataliotis, P., Tanaka, Y., Yannoutsos, N., Larsen, L., and Kioussis, D. (1991) Direct derivation of conditionally immortal cell lines from an *H-2K^b*-tsA58 transgenic mouse. *Proc. Natl. Acad. Sci. U.S.A.* **88**, 5096-5100
32. Kennedy, S. G., Wagner, A. J., Conzen, S. D., Jordán, J., Bellacosa, A., Tsichlis, P. N., and Hay, N. (1997) The PI 3-kinase/Akt signaling pathway delivers an anti-apoptotic signal. *Genes Dev.* **11**, 701-713
33. Eves, E. M., Xiong, W., Bellacosa, A., Kennedy, S. G., Tsichlis, P. N., Rosner, M. R., and Hay, N. (1998) Akt, a target of phosphatidylinositol 3-kinase, inhibits apoptosis in a differentiating neuronal cell line. *Mol. Cell. Biol.* **18**, 2143-2152
34. Rabinowitz, J. D., and Kimball, E. (2007) Acidic acetonitrile for cellular metabolome extraction from *E. coli*. *Anal. Chem.* **79**, 6167-6173
35. Chen, P., Liu, Z., Liu, S., Xie, Z., Aimiwu, J., Pang, J., Klisovic, R., Blum, W., Grever, M. R., Marcucci, G., and Chan, K. K. (2009) A LC-MS/MS method for the analysis of intracellular nucleoside triphosphate levels. *Pharm. Res.* **26**, 1504-1515

36. Gaidhu, M. P., Fediuc, S., and Ceddia, R. B. (2006) 5-Aminoimidazole-4-carboxamide-1-beta-D-ribofuranoside-induced AMP-activated protein kinase phosphorylation inhibits basal and insulin-stimulated glucose uptake, lipid synthesis, and fatty acid oxidation in isolated rat adipocytes. *J. Biol. Chem.* **281**, 25956–25964
37. King, T. D., Song, L., and Jope, R. S. (2006) AMP-activated protein kinase (AMPK) activating agents cause dephosphorylation of Akt and glycogen synthase kinase-3. *Biochem. Pharmacol.* **71**, 1637–1647
38. Lieberthal, W., Zhang, L., Patel, V. A., and Levine, J. S. (2011) AMPK protects proximal tubular cells from apoptosis induced by metabolic stress by an ATP-independent mechanism: potential role of Akt activation. *Am. J. Physiol. Renal Physiol.* **301**, F1177–F1192
39. Cai, S. L., Tee, A. R., Short, J. D., Bergeron, J. M., Kim, J., Shen, J., Guo, R., Johnson, C. L., Kiguchi, K., and Walker, C. L. (2006) Activity of TSC2 is inhibited by AKT-mediated phosphorylation and membrane partitioning. *J. Cell Biol.* **173**, 279–289
40. Dan, H. C., Sun, M., Yang, L., Feldman, R. I., Sui, X. M., Ou, C. C., Nellist, M., Yeung, R. S., Halley, D. J., Nicosia, S. V., Pledger, W. J., and Cheng, J. Q. (2002) Phosphatidylinositol 3-kinase/Akt pathway regulates tuberous sclerosis tumor suppressor complex by phosphorylation of tuberin. *J. Biol. Chem.* **277**, 35364–35370
41. Inoki, K., Li, Y., Zhu, T., Wu, J., and Guan, K. L. (2002) TSC2 is phosphorylated and inhibited by Akt and suppresses mTOR signalling. *Nat. Cell Biol.* **4**, 648–657
42. Sancak, Y., Thoreen, C. C., Peterson, T. R., Lindquist, R. A., Kang, S. A., Spooner, E., Carr, S. A., Sabatini, and D. M. (2007) PRAS40 is an insulin-regulated inhibitor of the mTORC1 protein kinase. *Mol. Cell* **25**, 903–915
43. Vander Haar, E., Lee, S. I., Bandhakavi, S., Griffin, T. J., and Kim, D. H. (2007) Insulin signalling to mTOR mediated by the Akt/PKB substrate PRAS40. *Nat. Cell Biol.* **9**, 316–323
44. Inoki, K., Li, Y., Zhu, T., Wu, J., and Guan, K. L. (2002) TSC2 is phosphorylated and inhibited by Akt and suppresses mTOR signalling. *Nat. Cell Biol.* **4**, 648–657
45. Corradetti, M. N., Inoki, K., Bardeesy, N., DePinho, R. A., and Guan, K. L. (2004) Regulation of the TSC pathway by LKB1: evidence of a molecular link between tuberous sclerosis complex and Peutz-Jeghers syndrome. *Genes Dev.* **18**, 1533–1538
46. Gwinn, D. M., Shackelford, D. B., Egan, D. F., Mihaylova, M. M., Mery, A., Vasquez, D. S., Turk, B. E., and Shaw, R. J. (2008) AMPK phosphorylation of raptor mediates a metabolic checkpoint. *Mol. Cell* **30**, 214–226
47. Shaw, R. J., Kosmatka, M., Bardeesy, N., Hurley, R. L., Witters, L. A., DePinho, R. A., and Cantley, L. C. (2004) The tumor suppressor LKB1 kinase directly activates AMP-activated kinase and regulates apoptosis in response to energy stress. *Proc. Natl. Acad. Sci. USA* **101**, 3329–3335
48. Racioppi, L., and Means, A. R. (2012) Calcium/calmodulin-dependent protein kinase kinase 2: roles in signaling and pathophysiology. *J. Biol. Chem.* **287**, 31658–31665
49. Hawley, S. A., Pan, D. A., Mustard, K. J., Ross, L., Bain, J., Edelman, A. M., Frenguelli, B. G., and Hardie, D. G. (2005) Calmodulin-dependent protein kinase kinase β is an alternative upstream kinase for AMP-activated protein kinase. *Cell Metab.* **2**, 9–19
50. Woods, A., Dickerson, K., Heath, R., Hong, S. P., Momcilovic, M., Johnstone, S. R., Carlson, M., and Carling, D. (2005) Ca^{2+} /calmodulin-dependent protein kinase kinase β acts upstream of AMP-activated protein kinase in mammalian cells. *Cell Metab.* **2**, 21–33
51. Anderson, K. A., Ribar, T. J., Lin, F., Noeldner, P. K., Green, M. F., Muehlbauer, M. J., Witters, L. A., Kemp, B. E., and Means, A. R. (2008) Hypothalamic CaMKK2 contributes to the regulation of energy balance. *Cell Metab.* **7**, 377–388
52. Fogarty, S., Hawley, S. A., Green, K. A., Saner, N., Mustard, K. J., and Hardie, D. G. (2010) Calmodulin-dependent protein kinase kinase- β activates AMPK without forming a stable complex: synergistic effects of Ca^{2+} and AMP. *Biochem. J.* **426**, 109–118
53. Wayman, G. A., Tokumitsu, H., and Soderling, T. R. (1997) Inhibitory cross-talk by cAMP

- kinase on the calmodulin-dependent protein kinase cascade. *J. Biol. Chem.* **272**, 16073–16076
54. Djouder, N., Tuerk, R. D., Suter, M., Salvioni, P., Thali, R. F., Scholz, R., Vaahtomeri, K., Auchli, Y., Rechsteiner, H., Brunisholz, R. A., Viollet, B., Mäkelä, T. P., Wallimann, T., Neumann, D., and Krek, W. (2010) PKA phosphorylates and inactivates AMPK α to promote efficient lipolysis. *EMBO J* **29**, 469–481
55. Feng, Z., Zhang, H., Levine, A. J., and Jin, S. (2005) The coordinate regulation of the p53 and mTOR pathways in cells. *Proc. Natl. Acad. Sci. USA* **102**, 8204–8209
56. Alexander, A., Cai, S.-L., Kim, J., Nanez, A., Sahin, M., MacLean, K. H., Inoki, K., Guan, K.-L., Shen, J., Person, M. D., Kusewitt, D., Mills, G. B., Kastan, M. B., and Walker, C. L. (2010) ATM signals to TSC2 in the cytoplasm to regulate mTORC1 in response to ROS. *Proc. Natl. Acad. Sci. USA* **107**, 4153–4158
57. Zmijewski, J. W., Banerjee, S., Bae, H., Friggeri, A., Lazarowski, E. R., and Abraham, E. (2010) Exposure to hydrogen peroxide induces oxidation and activation of AMP-activated protein kinase. *J. Biol. Chem.* **285**, 33154–33164

ACKNOWLEDGMENTS

We thank Dr. Zhong Li in the Metabolomics Laboratory of Roy J. Carver Biotechnology Center, University of Illinois at Urbana-Champaign, for the measurement of intracellular AMP, ADP, and ATP, and for invaluable discussion about the design and interpretation of experiments. We also thank Dr. Balaji Ganesh, Director, and Mr. Suresh Ramasamy, research specialist, in the Flow Cytometry Core Laboratory, University of Illinois at Chicago, for invaluable assistance in the design, acquisition, and analysis of the flow cytometry data presented in this publication. This paper is dedicated to the memory of Edith Levine.

FOOTNOTES

This work was supported, in whole or in part, by institutional funds from Dr. José A. Arruda and the Section of Nephrology, University of Illinois at Chicago (to J. S. L. and N. L.); National Center for Research Resources Grant S10RR024516 (for purchase of the 5500 QTRAP LC/MS/MS system); and operating grants (MOP-67101; MOP-97916) from the Canadian Institutes of Health Research (CIHR) (to J. R.)

FIGURE LEGENDS

FIGURE 1. Apoptotic targets inhibit the growth of BU.MPT responder cells. *A*, serum-starved BU.MPT responder cells were exposed to no targets (*Untreated*), apoptotic targets (*Apo*), or necrotic targets (*Nec*) at a target/responder cell ratio of 10:1 for 2 h. The source of apoptotic targets was actinomycin D-treated DO11.10 cells. Immediately prior to exposure (*0 hrs*) and at 24 h following exposure (*24 hrs*), relative cell size was determined by flow cytometric analysis of the forward scatter of responder cells in G1 phase of the cell cycle. *B*, the graph depicts the mean and S.E. from six separate flow cytometric analyses of the relative cell size of BU.MPT responder cells in G1 phase of the cell cycle. Within each analysis, experimental values were normalized to the mean forward scatter of control BU.MPT responders prior to target exposure (*0 hrs, Control*). $p < 0.02$, apoptotic targets *versus* no targets at 24 h; $p =$ not significant, necrotic targets *versus* no targets at 24 h. *Tar*, target(s). *Error bars (B)* denote S.E. *D*, an example of the gating procedure used to generate these data is provided for DAPI-stained BU.MPT responder cells exposed for 2 h to either no targets (upper panels) or apoptotic targets (lower panels), and analyzed 24 h later. The first gate (R1 in left panels) excludes cellular debris and/or dead cells ($< 2\times$ DNA content), and cellular aggregates (events to the right of the diagonal, where DAPI-area [DAPI-A] fluorescence exceeds DAPI-height [DAPI-H] fluorescence). The second gate (R2 in middle panels) comprises cells in G1 phase of the cell cycle ($2\times$ DNA content). The relative size of responders within R2 was determined by measuring forward scatter (FSC Area). The overlay in the right panel compares the relative size of responders exposed to no targets (blank fill) *versus* those exposed to apoptotic targets (crosshatched fill).

FIGURE 2. Apoptotic targets inhibit the phosphorylation and activity of p70S6K in BU.MPT responder cells. Serum-starved BU.MPT responder cells were stimulated with either (*A*) apoptotic targets (*Apo cells*) or (*B*) necrotic targets (*Nec cells*) at a target/responder cell ratio ranging from 1:1 to 1:32 in 2-fold serial dilutions, as indicated by the *schematic*. The source of apoptotic targets was staurosporine-treated BU.MPT cells. For studies without EGF (top panel in *A* and *B*), target stimulation was for 15 min. For studies with EGF (bottom panel in *A* and *B*), BU.MPT responders were exposed to targets for 30 min, followed by a 15-min stimulation with EGF (50 nM). In all cases, targets and non-adherent responder cells were removed by washing, and BU.MPT responder cell lysates were probed with anti-phosphorylated p70S6K and S6 antibodies as shown. Equal loading was confirmed by probing for total p70S6K. Shown is a representative set of blots from five separate experiments. Gaps between lanes exist for clarity of presentation or because lanes were non-contiguous on the original immunoblot. *C*, densitometric quantitation of the effects of apoptotic targets, using total p70S6K as a loading control, is provided. $p < 0.05$ for the following conditions: apoptotic targets *versus* no targets for all apoptotic target: responder cell ratios at or greater than 1:4 (p70S6K no EGF), 1:8 (p70S6K + EGF), 1:8 (S6 no EGF), and 1:8 (S6 + EGF).

FIGURE 3. Apoptotic targets activate AMPK and inhibit Akt in BU.MPT responder cells. Serum-starved BU.MPT responder cells were stimulated with either apoptotic targets (*Apo cells*) or necrotic targets (*Nec cells*) at a target/responder cell ratio ranging from 1:1 to 1:32 in 2-fold serial dilutions, as indicated by the *schematic*. The source of apoptotic targets was staurosporine-treated BU.MPT cells. For studies without EGF (top panel in *A* and *B*), target stimulation was for 15 min. For studies with EGF (bottom panel in *A* and *B*), responders were exposed to targets for 30 min, followed by a 15-min stimulation with EGF (50 nM). In all cases, targets and non-adherent BU.MPT responders were removed by washing, and BU.MPT responder cell lysates were probed with (*A*) anti-phosphorylated AMPK- α chain antibodies or (*B*) anti-phosphorylated Akt, GSK3 α/β , FoxO1, and FoxO3a antibodies as shown. Equal loading was confirmed by probing for total β -actin. Shown is a representative set of blots from five separate experiments. Gaps between lanes exist for clarity of presentation or because lanes were non-contiguous on the original immunoblot. *C*, *D*, *E*, densitometric quantitation of the effects of apoptotic

targets, using total β -actin as a loading control, is provided. $p < 0.05$ for the following conditions: apoptotic targets *versus* no targets for all apoptotic target: responder cell ratios at or greater than 1:32 (AMPK no EGF), 1:16 (AMPK + EGF), 1:1 (Akt-T308 no EGF), 1:4 (Akt-T308 + EGF), 1:2 (Akt-S473 no EGF), 1:8 (Akt-S473 + EGF), 1:32 (GSK3 α/β no EGF), 1:32 (GSK3 α/β + EGF), 1:32 (FoxO1 no EGF), 1:8 (FoxO1 + EGF), 1:1 (FoxO3a no EGF), and 1:2 (FoxO3a + EGF).

FIGURE 4. Pharmacological inhibition of AMPK prevents inhibition of p70S6K and cell growth by apoptotic targets. *A*, serum-starved BU.MPT responder cells were pretreated for 2 h with vehicle or compound C at the indicated concentrations, following which they were stimulated with either apoptotic (*Apo*) targets or necrotic (*Necro*) targets at a target/responder cell ratio of 1:1 for 30 min, washed, incubated for a further 15 min, and then harvested. The source of apoptotic targets was staurosporine-treated BU.MPT cells. In all cases, targets and non-adherent responder cells were removed by washing, and BU.MPT responder cell lysates were probed with anti-phosphorylated AMPK- α chain, p70S6K, S6, and GSK3 α/β antibodies as shown. Equal loading was confirmed by probing for total AMPK β 1/ β 1. Shown is a representative set of blots from three separate experiments. Gaps between lanes exist for clarity of presentation or because lanes were non-contiguous on the original immunoblot. *B*, serum-starved BU.MPT responder cells were pretreated with vehicle or compound C (10 μ M) for 2 h, then exposed to no targets (*Untreated*), apoptotic (*Apo*) targets, or necrotic (*Nec*) targets at a target/responder cell ratio of 10:1 for 2 h. The source of apoptotic targets was actinomycin D-treated DO11.10 cells. At 24 h following exposure, relative cell size was determined by flow cytometric analysis of the forward scatter of responder cells in G1 phase of the cell cycle. *C*, the graph depicts the mean and S.E. from three separate flow cytometric analyses of the relative cell size of BU.MPT responder cells in G1 phase of the cell cycle. Within each analysis, experimental values were normalized to the mean forward scatter of BU.MPT responders exposed to no targets (*Control*) in the absence of compound C. $p < 0.05$, apoptotic targets *versus* no targets, in the absence of compound C; $p < 0.02$, apoptotic targets in presence *versus* absence of compound C. *Tar*, target(s). *Error bars* (*C*) denote S.E. *D*, densitometric quantitation, using total AMPK β 1/ β 1 as a loading control, is provided for the immunoblots shown in *A*. $p < 0.05$ for the following conditions: apoptotic targets *versus* no targets for AMPK α -T172 and GSK3 α/β -S21/9 (in either the absence or the presence of all concentrations of compound C), and for p70S6K-T389 and S6-S240/244 (only in the absence of compound C). $p =$ not significant for the following conditions: apoptotic targets *versus* no targets for p70S6K-T389 and S6-S240/244, in the presence of all concentrations of compound C.

FIGURE 5. Molecular inhibition of AMPK prevents inhibition of p70S6K and cell growth by apoptotic targets. *A*, serum-starved BU.MPT responder cells, untransduced (–) or stably transduced with either control scrambled (*Scrambled*) or β 1-AMPK (β 1-AMPK) shRNA, were stimulated with apoptotic targets (*Apo*) or necrotic targets (*Necro*) at a target/responder cell ratio of 1:1 for 30 min, washed, incubated for a further 15 min, and then harvested. The source of apoptotic targets was staurosporine-treated BU.MPT cells. In all cases, targets and non-adherent responder cells were removed by washing, and BU.MPT responder cell lysates were probed with anti-phosphorylated AMPK- α chain, p70S6K, S6, and GSK3 α/β and anti-total AMPK β 1/ β 1 antibodies as shown. Equal loading was confirmed by probing for total GAPDH. Shown is a representative set of blots from three separate experiments. Gaps between lanes exist for clarity of presentation or because lanes were non-contiguous on the original immunoblot. *B*, serum-starved BU.MPT responder cells, stably transduced with either control scrambled (*Scrambled*) or β 1-AMPK (β 1-AMPK) shRNA, were exposed to no targets (*Untreated*) or apoptotic targets (*Apo*) at a target/responder cell ratio of 10:1 for 6 h. The source of apoptotic targets was actinomycin D-treated DO11.10 cells. At 24 h following exposure, relative cell size was determined by flow cytometric analysis of the forward scatter of responder cells in G1 phase of the cell cycle. *C*, the graph depicts the mean and S.E. from four separate flow cytometric analyses of the relative cell size of BU.MPT responder cells in G1 phase of the cell cycle. Within each analysis, experimental values were normalized to the mean

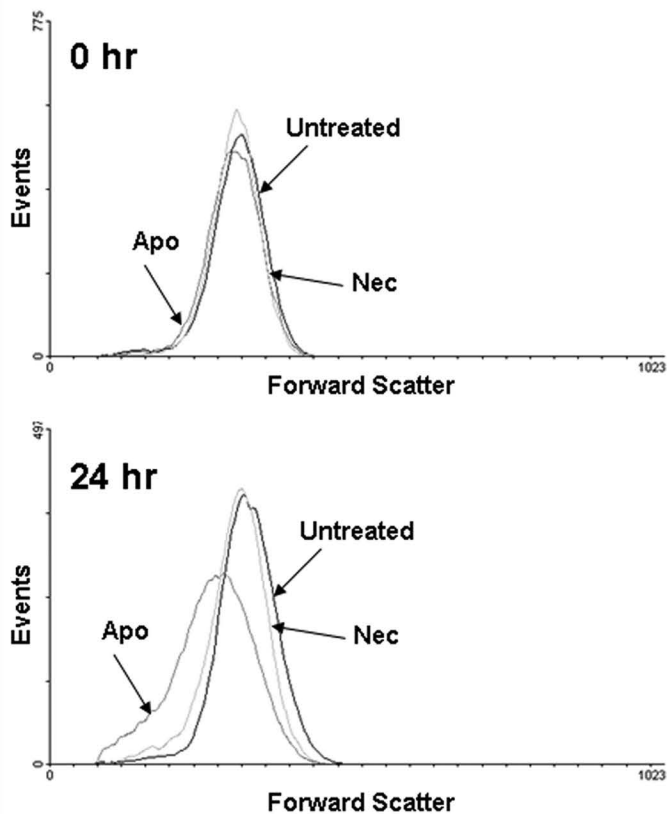
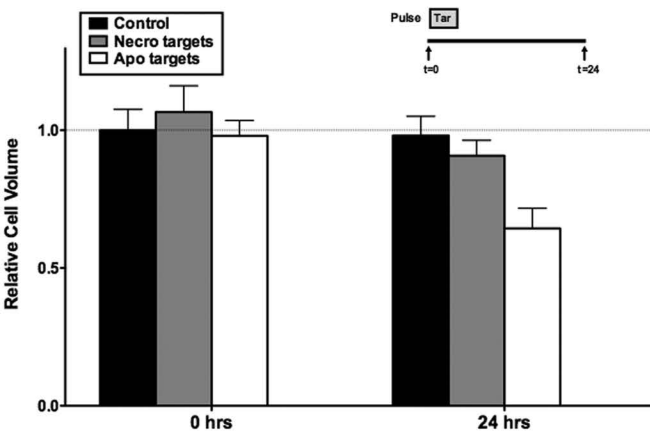
forward scatter of BU.MPT responders, expressing either scrambled or $\beta 1$ -AMPK shRNA, not exposed to targets (*No targets*). $p < 0.01$, apoptotic targets *versus* no targets, scrambled shRNA; $p < 0.03$, apoptotic targets *versus* no targets, $\beta 1$ -AMPK shRNA; $p < 0.02$, scrambled *versus* $\beta 1$ -AMPK shRNA, apoptotic targets. *Error bars* (C) denote S.E. D, densitometric quantitation, using total GAPDH as a loading control, is provided for the immunoblots shown in A. $p < 0.05$ for the following conditions: apoptotic targets *versus* no targets for AMPK α -T172, p70S6K-T389, and S6-S240/244, in untransduced and scrambled shRNA-transduced responders; and for GSK3 α/β -S21/9 in untransduced, scrambled shRNA-transduced, and $\beta 1$ -AMPK-transduced responders. $p =$ not significant for the following conditions: apoptotic targets *versus* no targets for AMPK α -T172, p70S6K-T389, and S6-S240/244 in $\beta 1$ -AMPK-transduced responders.

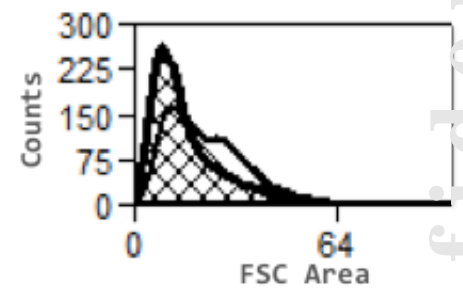
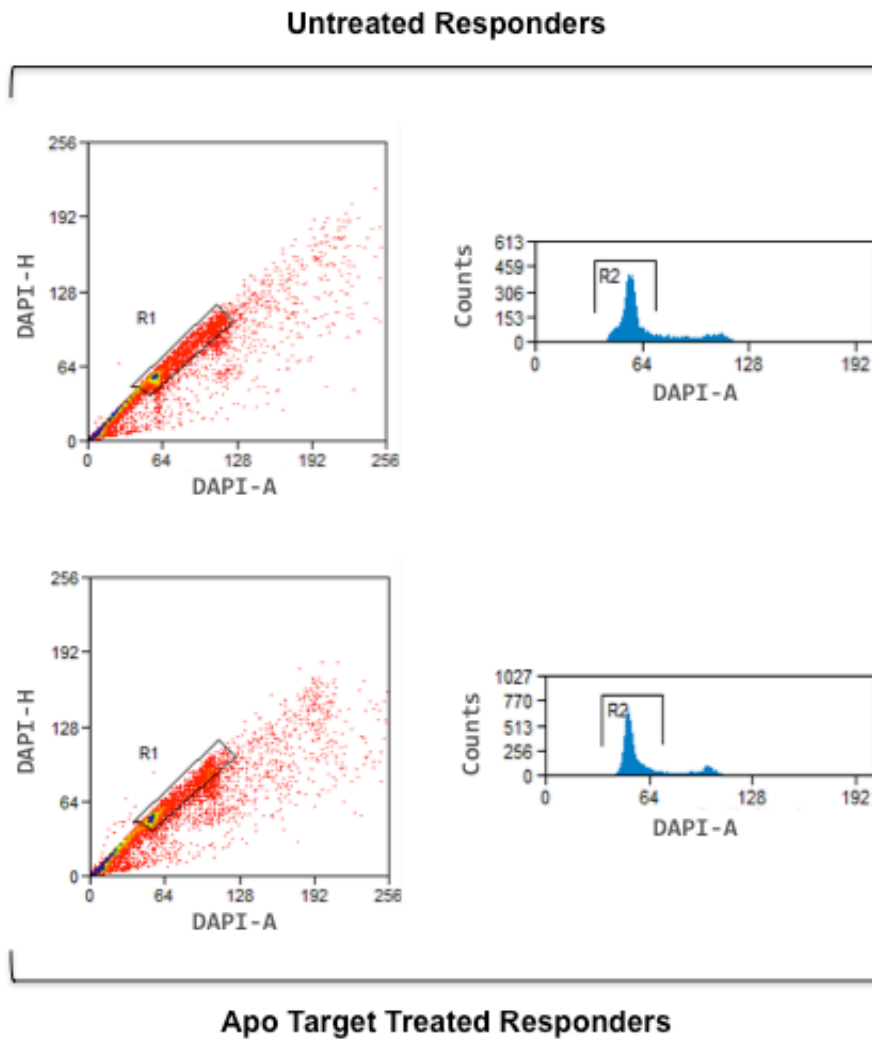
FIGURE 6. Constitutive activation of Akt prevents inhibition of p70S6K and cell growth by apoptotic targets. A, B, serum-starved BU.MPT responder cells, infected with retroviral constructs containing either GFP alone (*GFP*) or GFP plus constitutively active Akt (*myrAkt-GFP*), were stimulated with no targets (–) or apoptotic (*Apo*) targets at a target/responder cell ratio of 1:1 or 1:4 for 30 min in the absence or presence of compound C (20 μ M), washed, incubated for a further 15 min, and then harvested. The source of apoptotic targets was staurosporine-treated BU.MPT cells. In all cases, targets and non-adherent responder cells were removed by washing, and BU.MPT responder cell lysates were probed with (A) anti-phosphorylated Akt antibodies or (B) anti-phosphorylated AMPK- α chain, p70S6K, S6, and GSK3 α/β antibodies as shown. Equal loading was confirmed by probing for either (A) total GAPDH or (B) total AMPK $\beta 1/\beta 1$. Shown is a representative set of blots from three separate experiments. Gaps between lanes exist for clarity of presentation or because lanes were non-contiguous on the original immunoblot. C, serum-starved BU.MPT responder cells, infected with retroviral constructs containing either GFP alone (*GFP*) or GFP plus constitutively active Akt (*myrAkt-GFP*), were exposed to no targets, apoptotic (*Apo*) targets, or necrotic (*Necro*) targets at a target/responder cell ratio of 10:1 for 2 h, in the absence (*Control*) or presence of compound C (10 μ M). The source of apoptotic targets was actinomycin D-treated DO11.10 cells. At 24 h following exposure, relative cell size was determined by flow cytometric analysis of the forward scatter of responder cells in G1 phase of the cell cycle. D, the graph depicts the mean and S.E. from six separate flow cytometric analyses of the relative cell size of BU.MPT responder cells in G1 phase of the cell cycle. Within each analysis, experimental values were normalized to the mean forward scatter of BU.MPT responders expressing GFP alone (*GFP*) immediately prior to target exposure at 0 h. $p < 0.001$, apoptotic targets *versus* no targets, GFP; $p < 0.05$, apoptotic targets *versus* no targets, myrAkt-GFP; $p < 0.05$, GFP *versus* myrAkt-GFP, apoptotic targets. *Tar*, target(s). *Error bars* (D) denote S.E. E, densitometric quantitation, using total AMPK $\beta 1/\beta 1$ as a loading control, is provided for the immunoblots shown in B. $p < 0.05$ for the following conditions: apoptotic targets *versus* no targets in control GFP-transfected responders for S6-S240/244 and GSK3 α/β -S21/9 at apoptotic target: responder cell ratios of 1:1 and 1:4; and in control GFP-transfected responders for AMPK α -T172 and p70S6K-T389 at an apoptotic target: responder cell ratio of 1:1. $p =$ not significant for the following conditions: apoptotic targets *versus* no targets in myrAkt-GFP-transfected responders for AMPK α -T172, p70S6K-T389, S6-S240/244, and GSK3 α/β -S21/9 at all apoptotic target: responder cell ratios, regardless of the presence or the absence of compound C.

FIGURE 7. Apoptotic targets activate AMPK and inhibit cell growth independently of changes in intracellular energy stores. Serum-starved BU.MPT responder cells were exposed to no targets (*Control*), apoptotic (*Apo*) targets, or necrotic (*Necro*) targets at a target/responder ratio of 10:1 for 30 min. Targets and non-adherent responder cells were washed away. After an additional 0.5 h or 18 h, the intracellular content of AMP, ADP, and ATP in BU.MPT responder cell lysates was determined by liquid chromatography-tandem mass spectrometry (LC-MS/MS). For each experimental condition, the following calculated ratios are shown: the concentration of ADP to that of ATP (*ADP:ATP ratio*); the concentration of AMP to that of ATP (*AMP:ATP ratio*); and the number of adenylate-bound high energy

phosphate bonds present compared to the maximum number of high energy bonds possible (energy charge). As shown by the y-axis, all three ratios are dimensionless numbers between 0 and 1. The targets were actinomycin D-treated DO11.10 cells. The graphs depict the mean and S.E. from three separate experiments. p = not significant for the following conditions: apoptotic targets *versus* no targets, for ADP:ATP ratio, AMP:ATP ratio, and energy charge at both 0.5 h and 18 h. *Error bars (D)* denote S.E.

FIGURE 8. The effects of apoptotic targets on BU.MPT responder cell growth are dependent on cell-cell interaction but independent of phagocytosis. *A*, serum-starved BU.MPT responder cells were exposed to no targets or apoptotic (*Apo*) targets at a target/responder cell ratio of 10:1 for 2 h, as indicated by the *schematic*, either unimpeded, enabling direct target-responder physical interaction (*Control*), or with separation of targets and responders by a 0.4 μ M polycarbonate membrane in a Transwell® permeable support system (*Transwell*). *B*, serum-starved BU.MPT responder cells, pretreated with vehicle or cytochalasin D (*Cytochalasin*), an inhibitor of phagocytosis, at the indicated concentrations, were exposed to no targets or apoptotic (*Apo*) targets at a target/responder cell ratio of 10:1 for 2 h, as indicated by the *schematic*. *A*, *B*, the source of apoptotic targets was actinomycin D-treated DO11.10 cells. At 24 h following exposure, relative cell size was determined by flow cytometric analysis of the forward scatter of responder cells in G1 phase of the cell cycle. The graph depicts the mean and S.E. from three separate flow cytometric analyses of the relative cell size of BU.MPT responder cells in G1 phase of the cell cycle. Within each analysis, experimental values were normalized to the mean forward scatter of control BU.MPT responders exposed to no apoptotic targets, in the absence of (*A*) a transwell support system or (*B*) cytochalasin D. *Error bars (A, B)* denote S.E.

A**B**



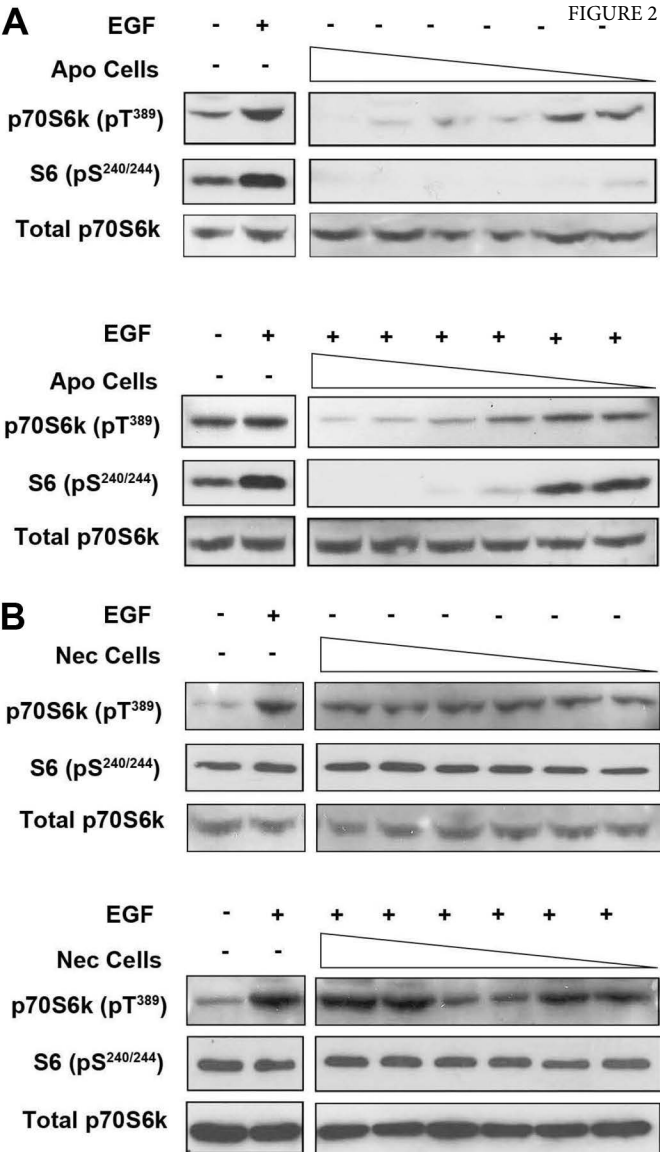
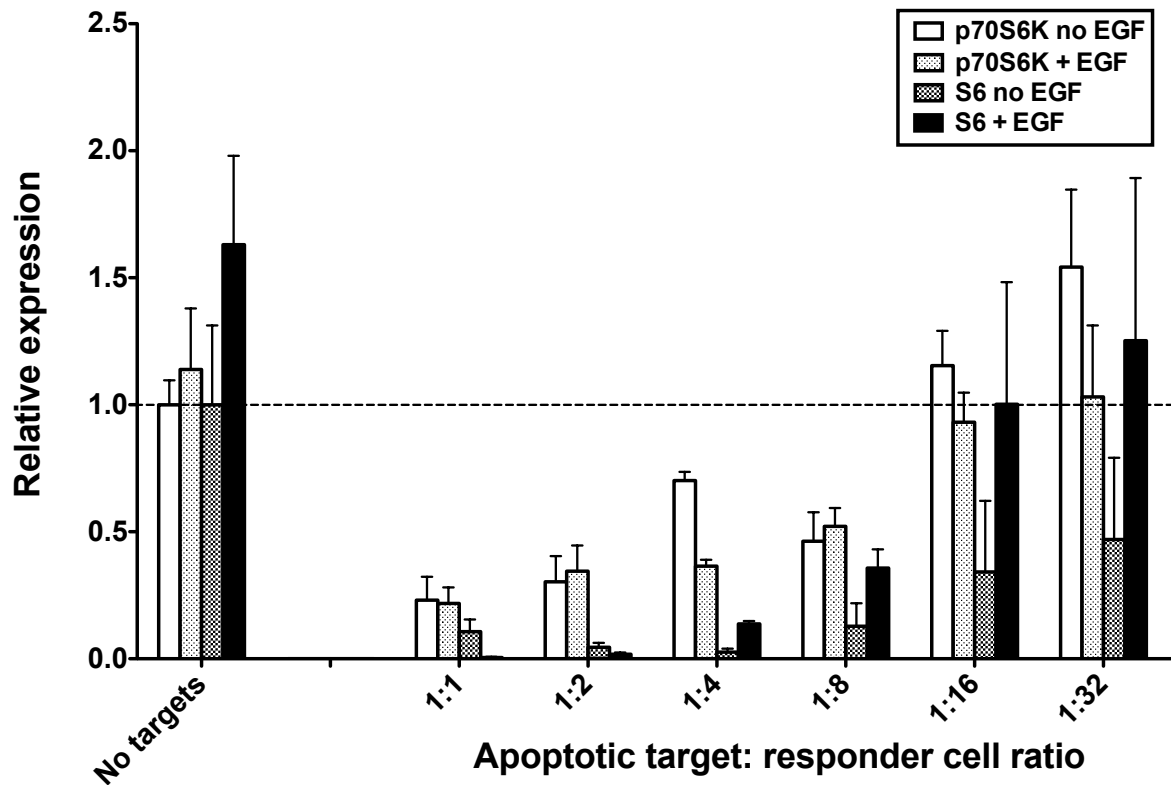


FIGURE 2C



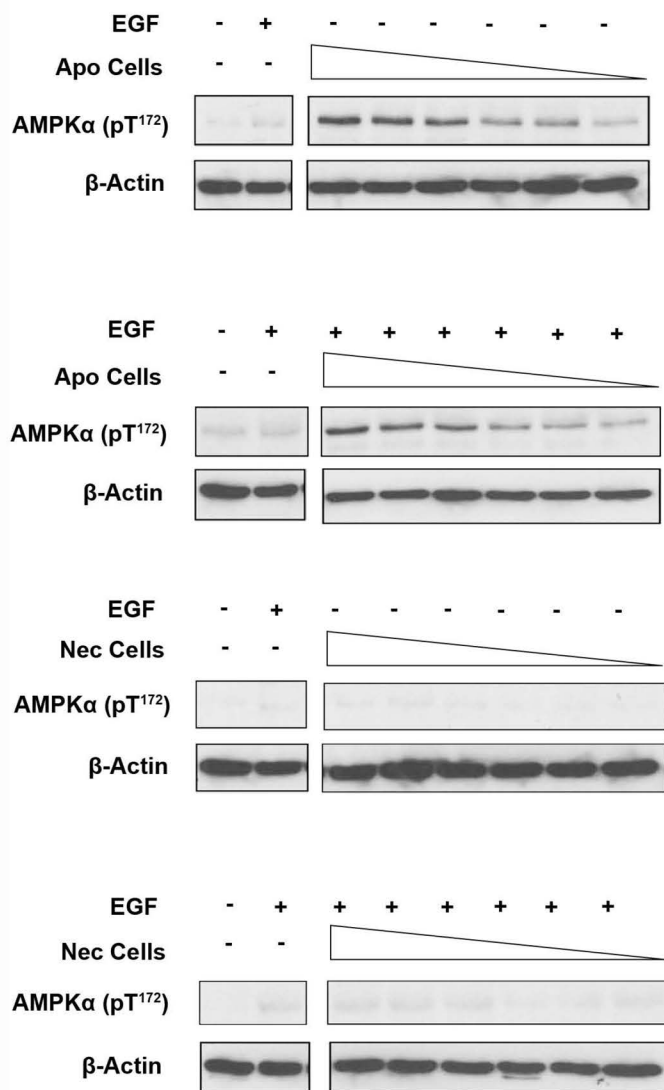
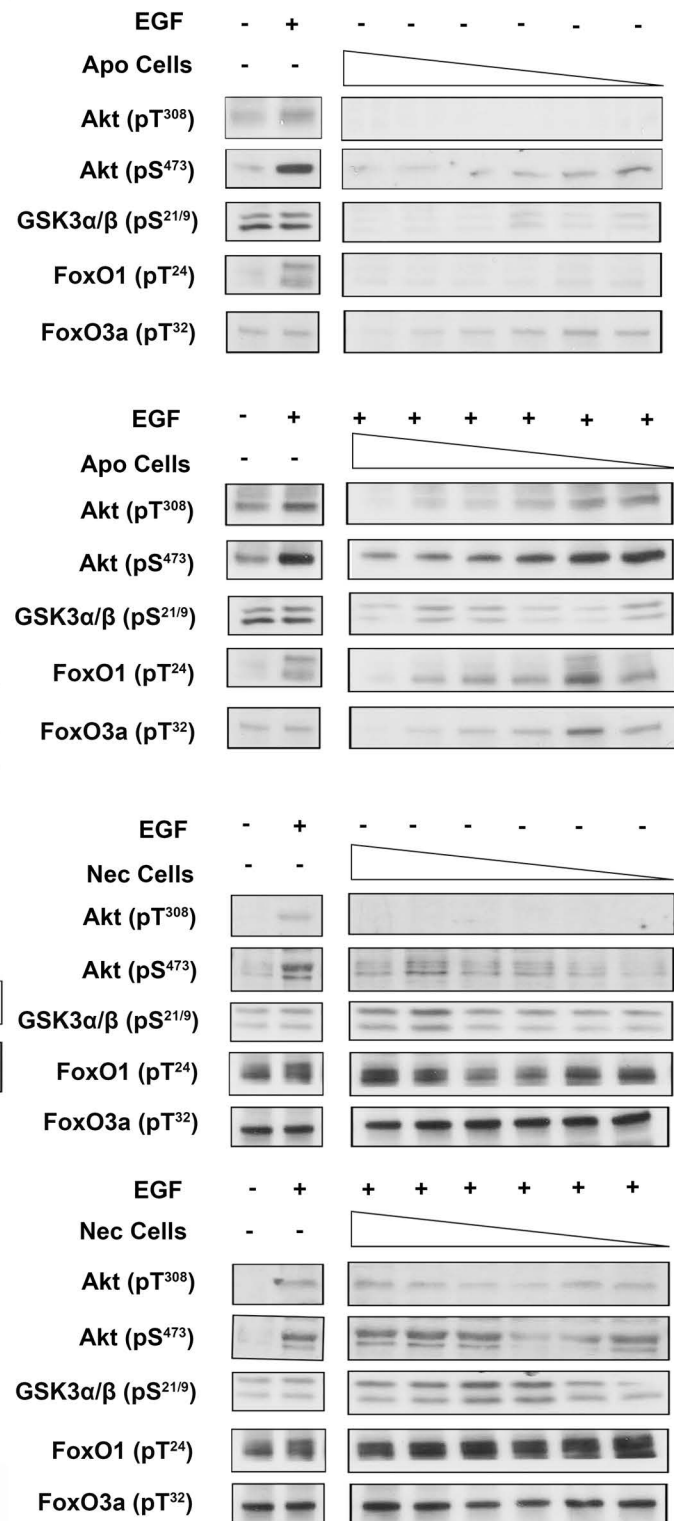
A**B**

FIGURE 3C

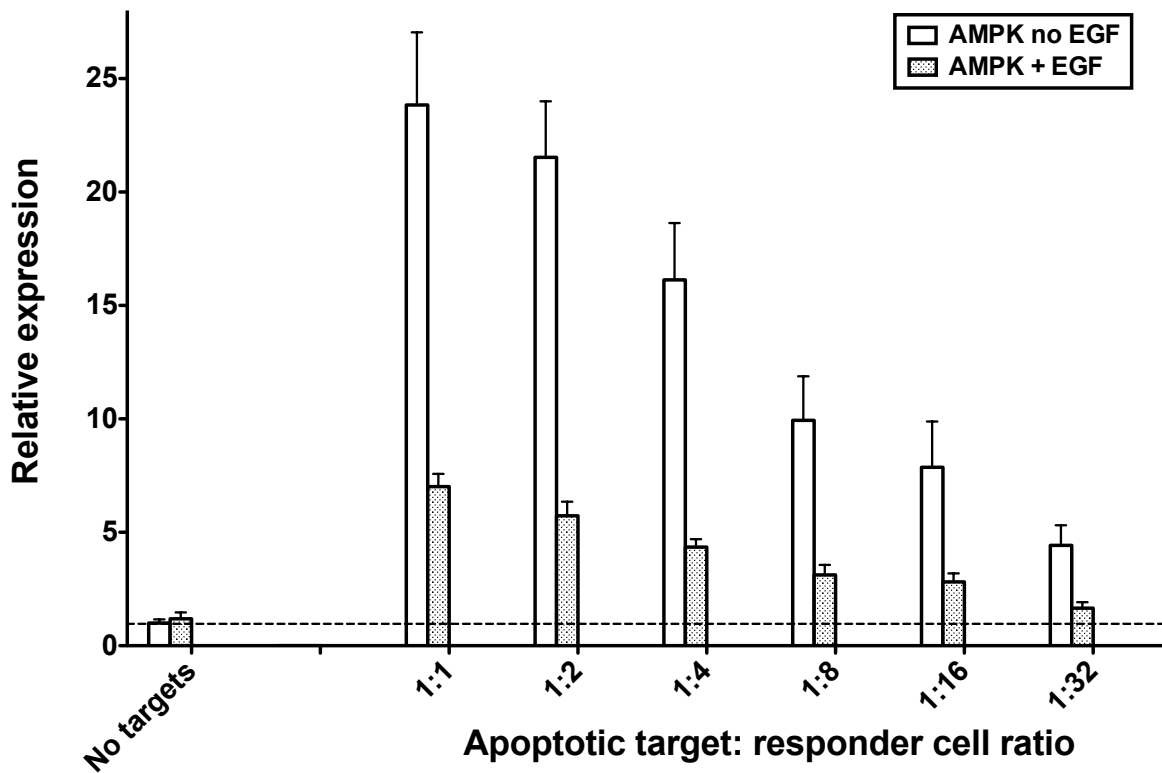


FIGURE 3D

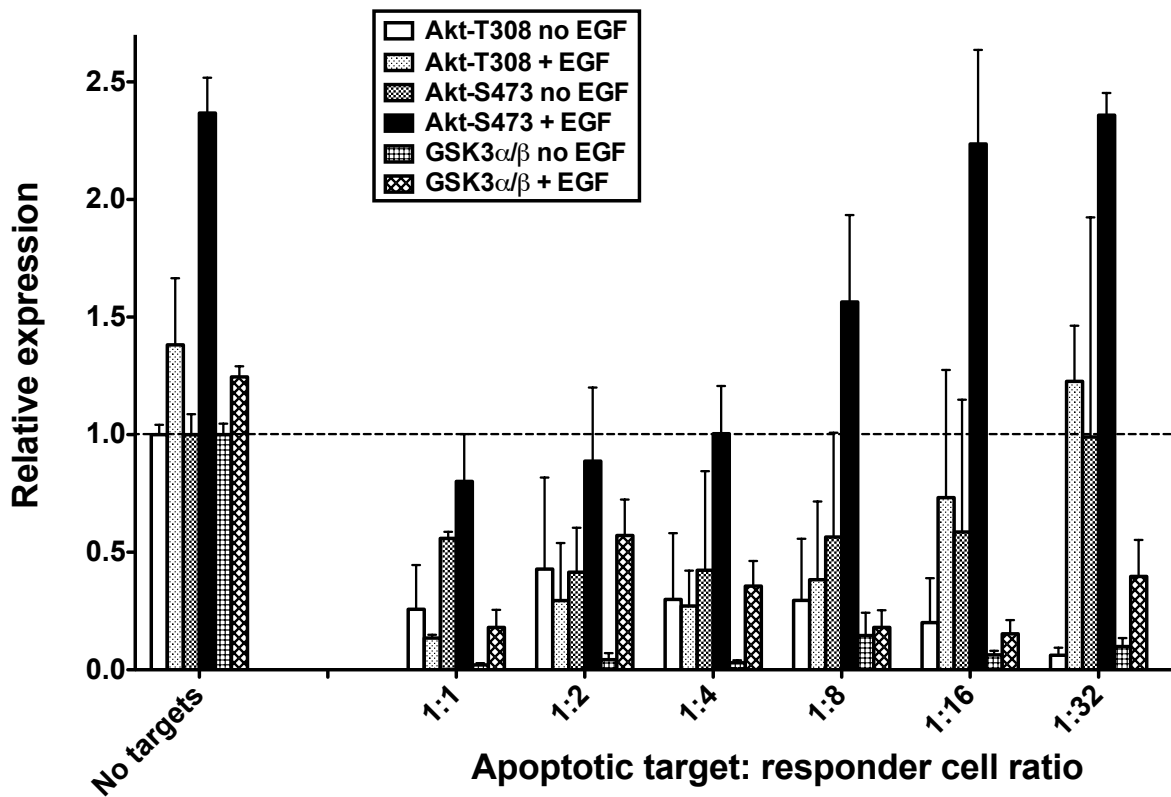
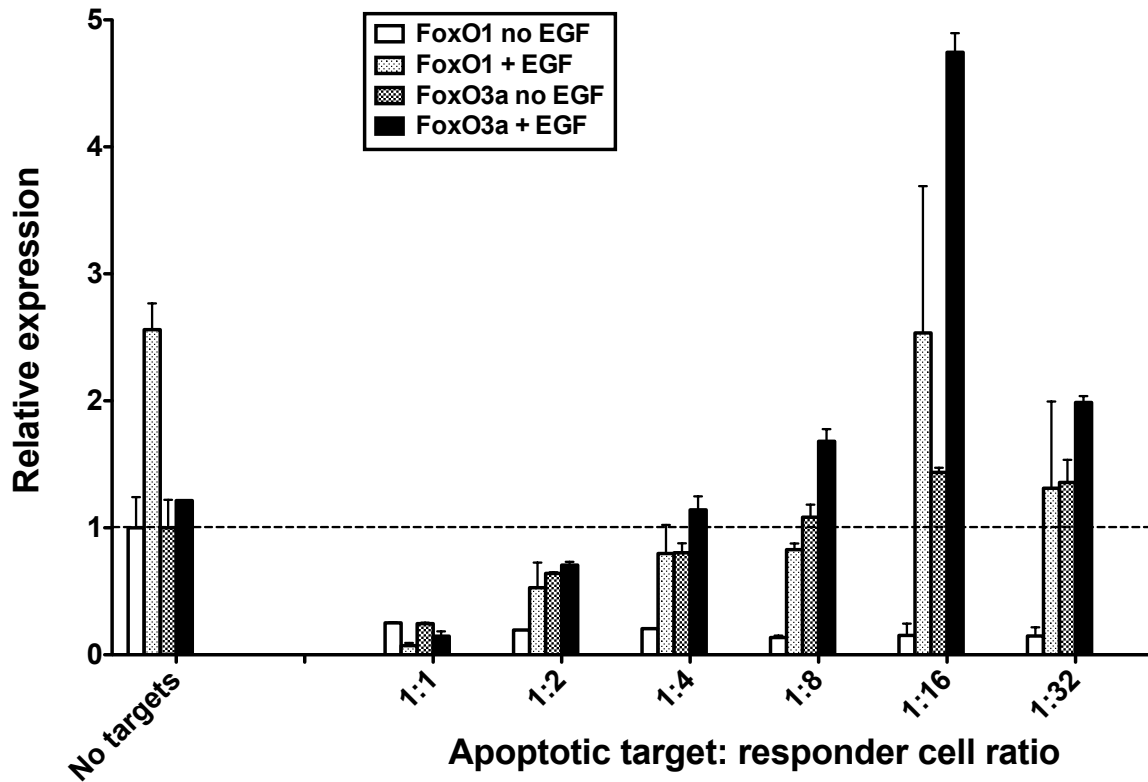
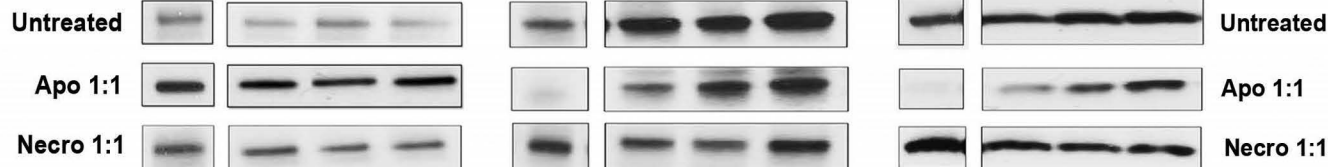
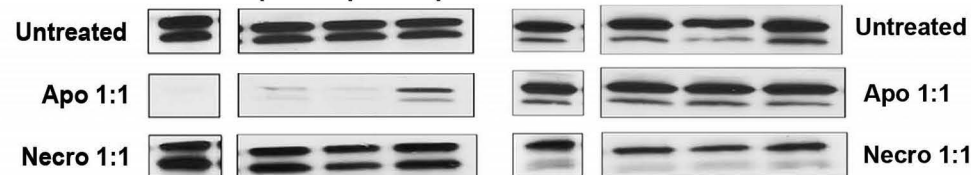
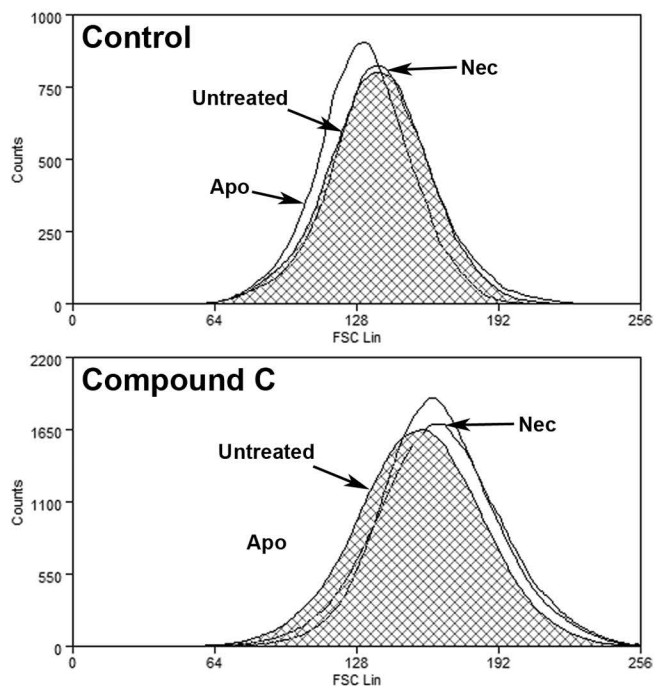
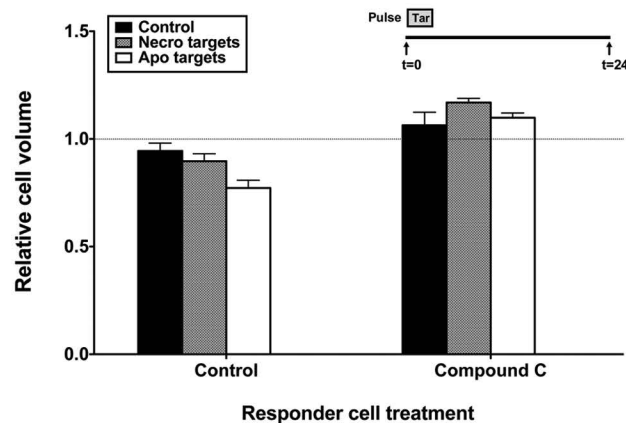
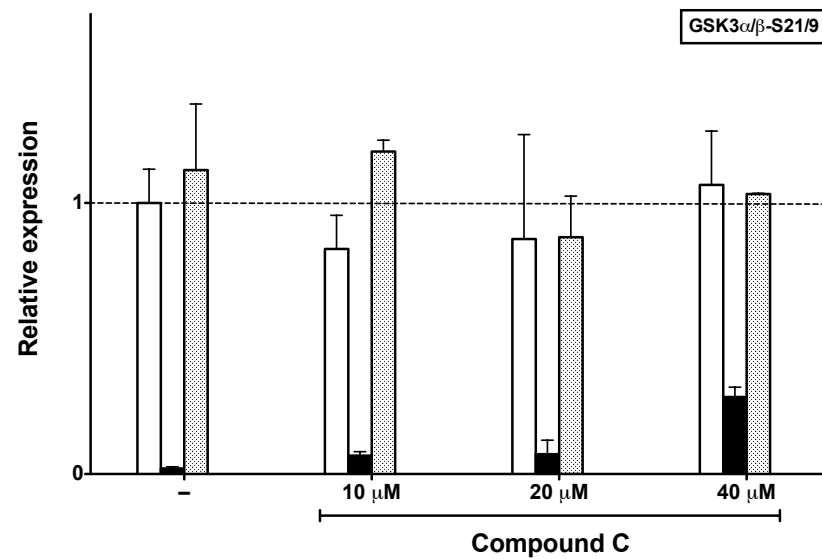
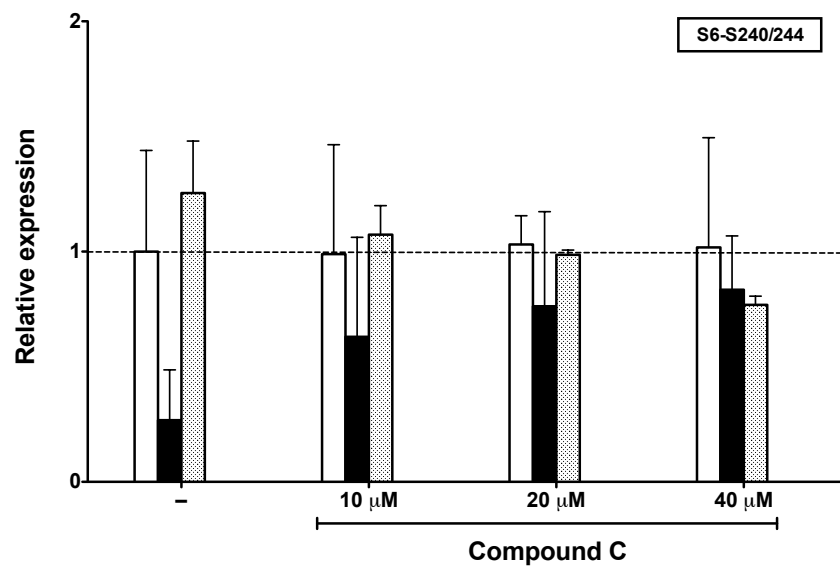
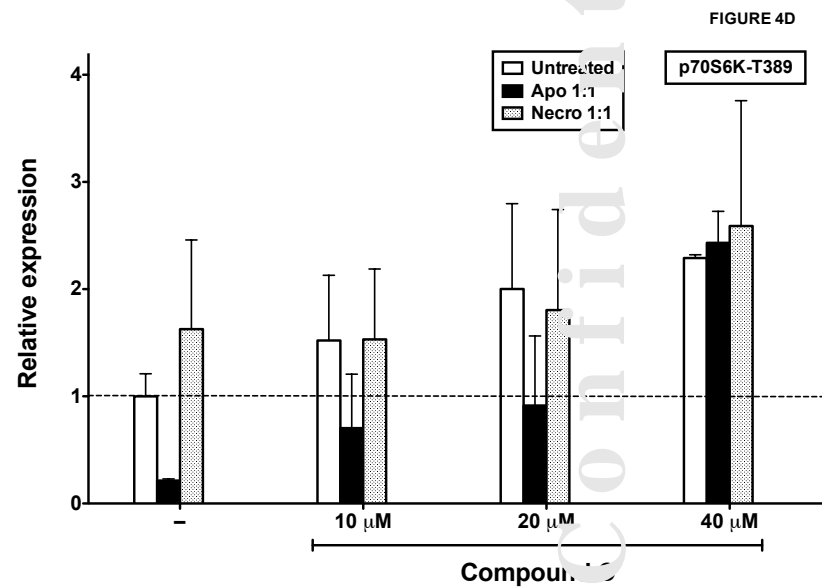
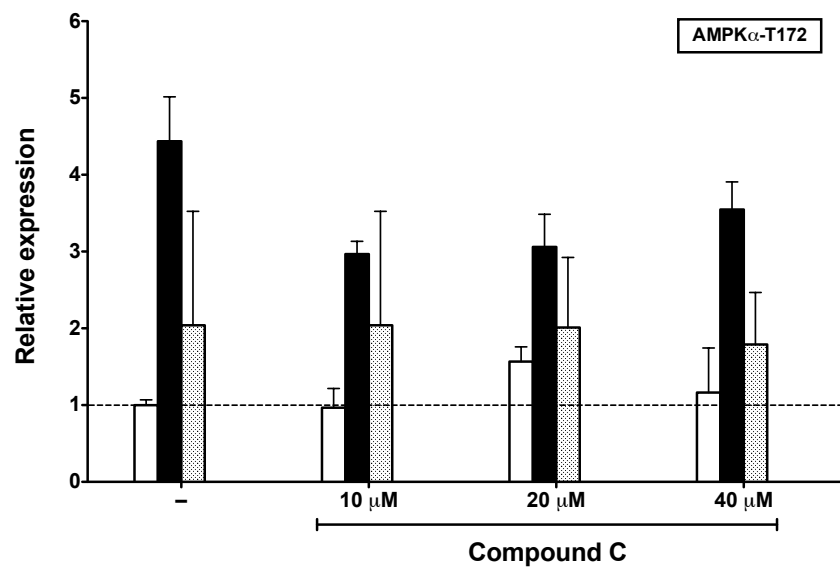
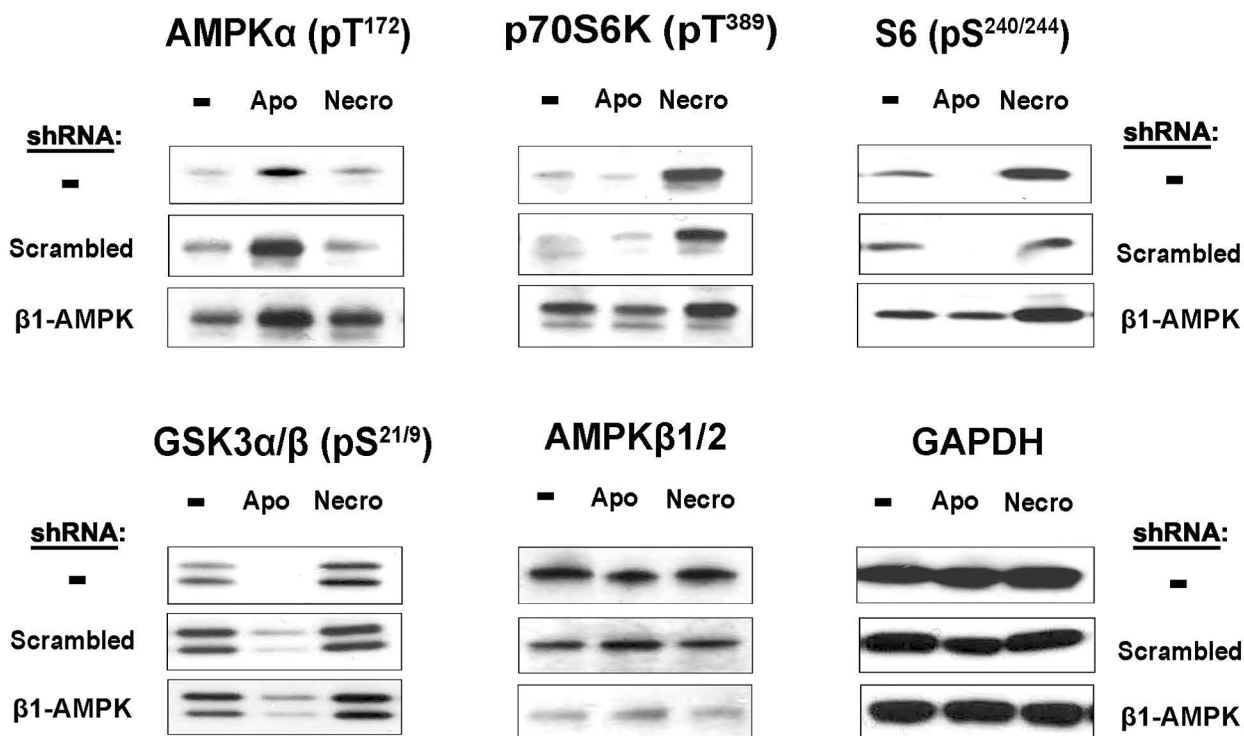
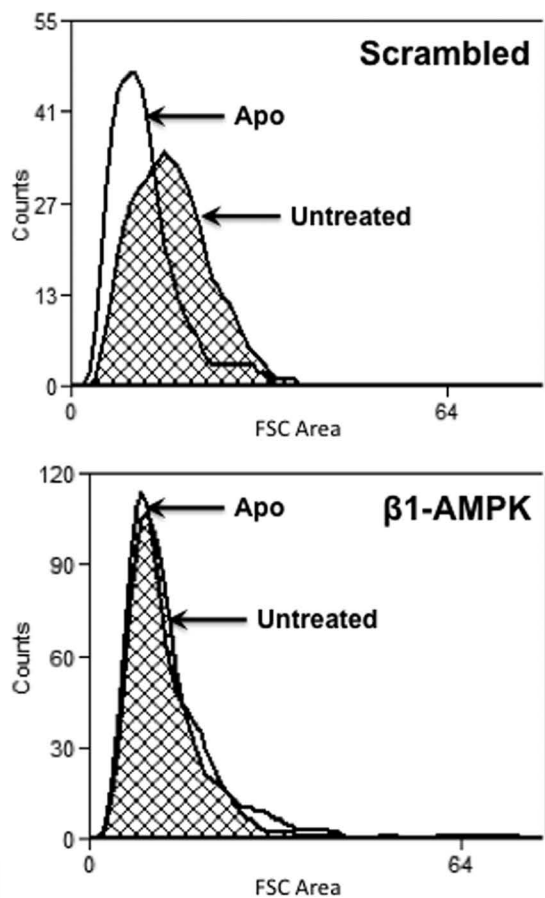
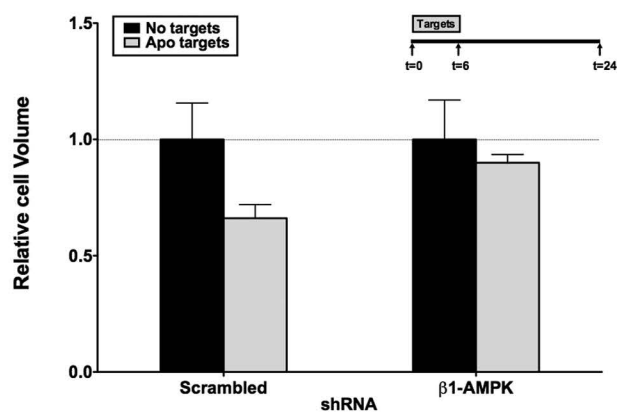


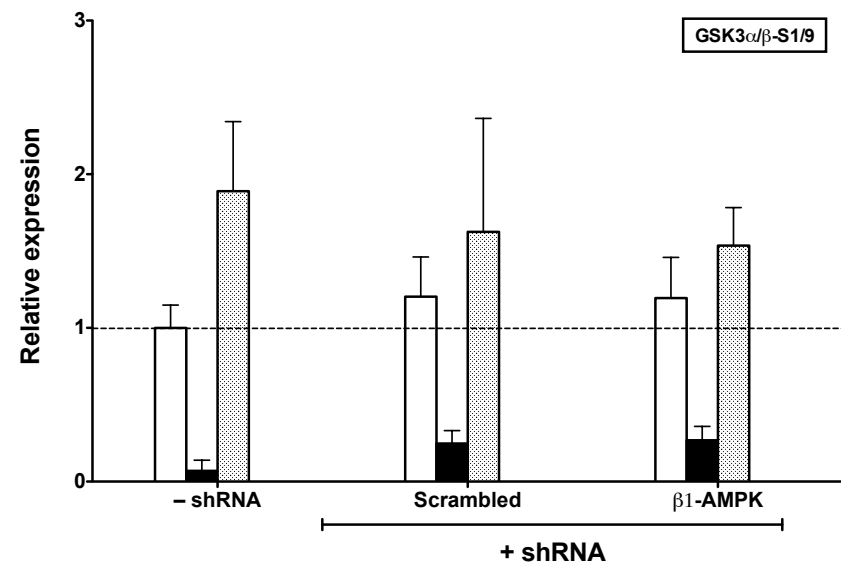
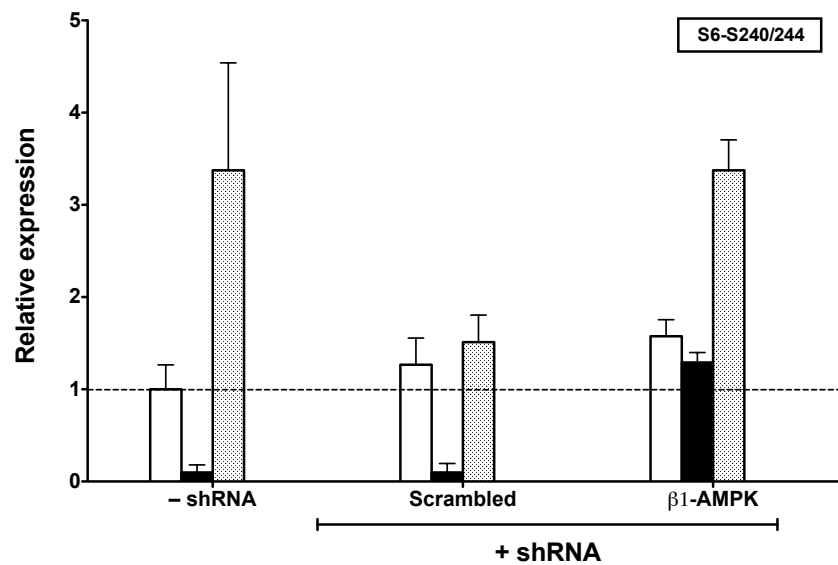
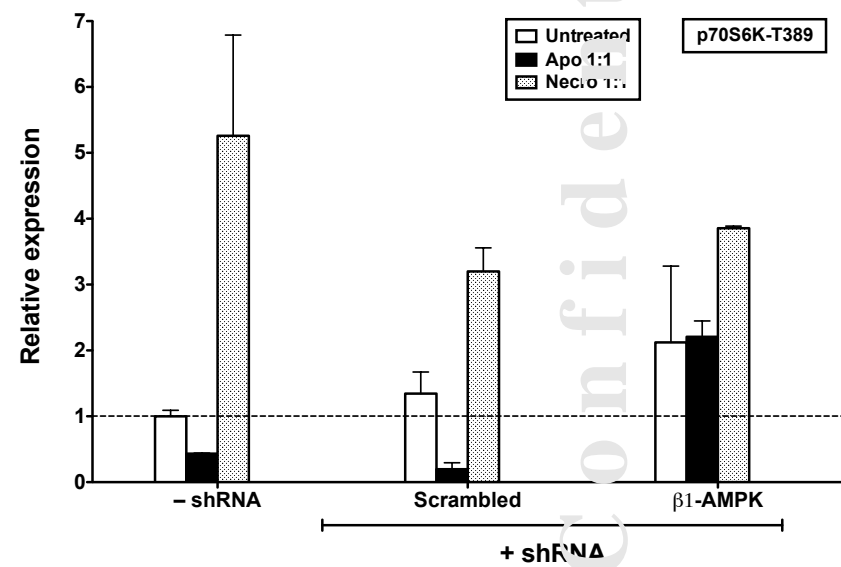
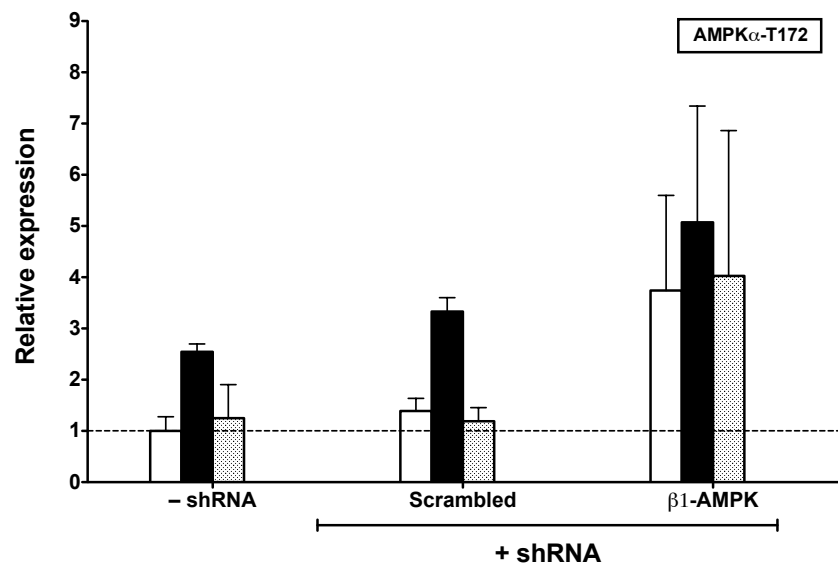
FIGURE 3E

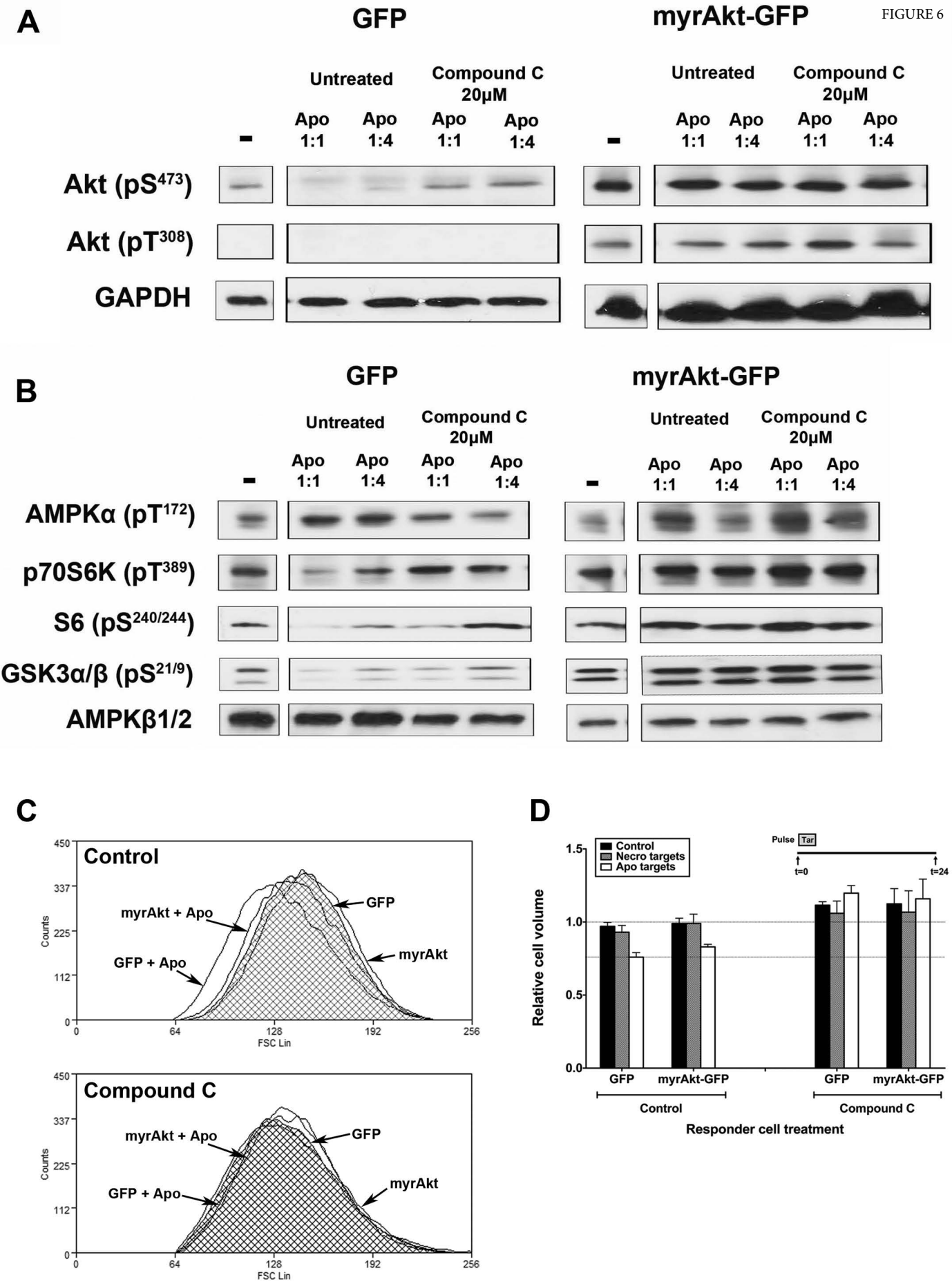


A**AMPK α (pT¹⁷²)****p70S6K (pT³⁸⁹)****S6 (pS^{240/244})**Compound C
- 10 μ M 20 μ M 40 μ MCompound C
- 10 μ M 20 μ M 40 μ MCompound C
- 10 μ M 20 μ M 40 μ M**GSK3 α/β (pS^{21/9})****AMPK β 1/2**Compound C
- 10 μ M 20 μ M 40 μ MCompound C
- 10 μ M 20 μ M 40 μ M**B****C**



A**B****C**





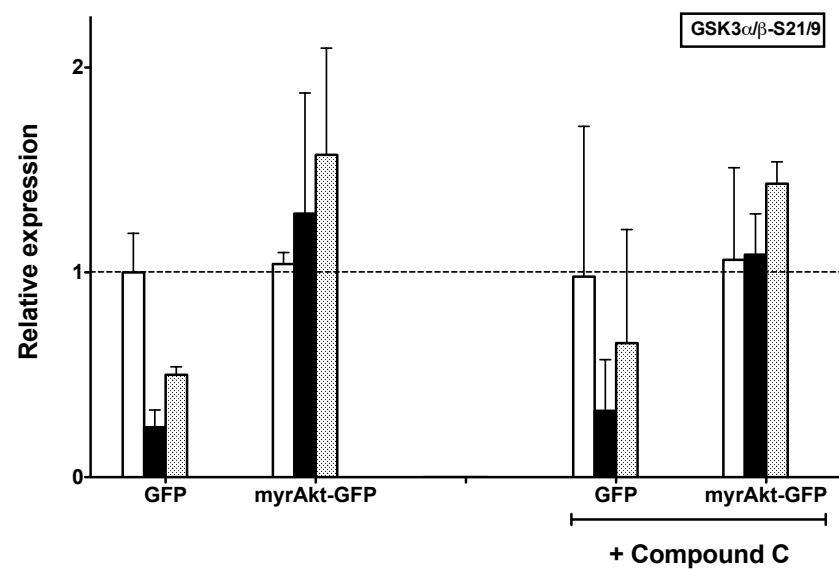
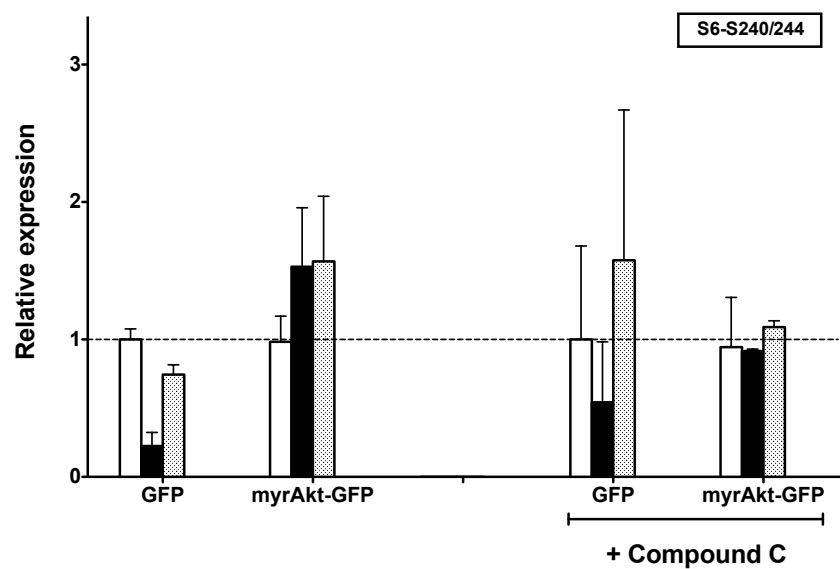
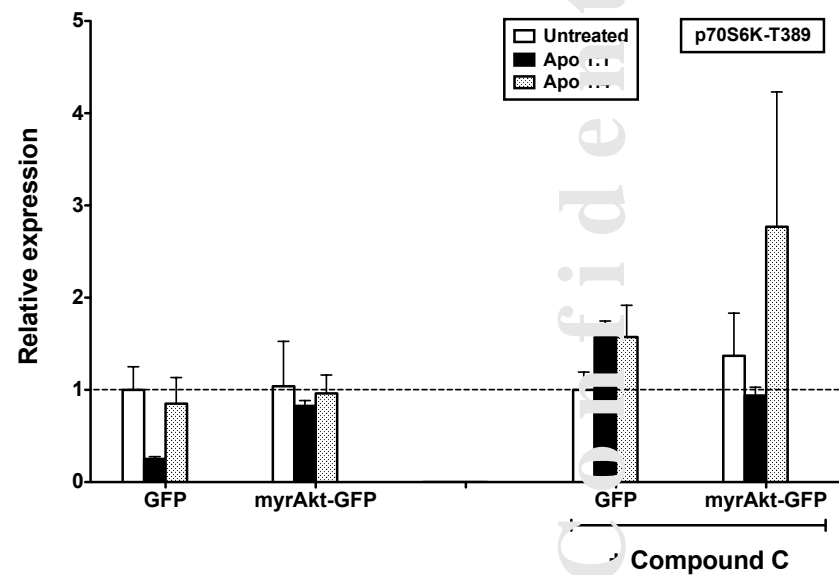
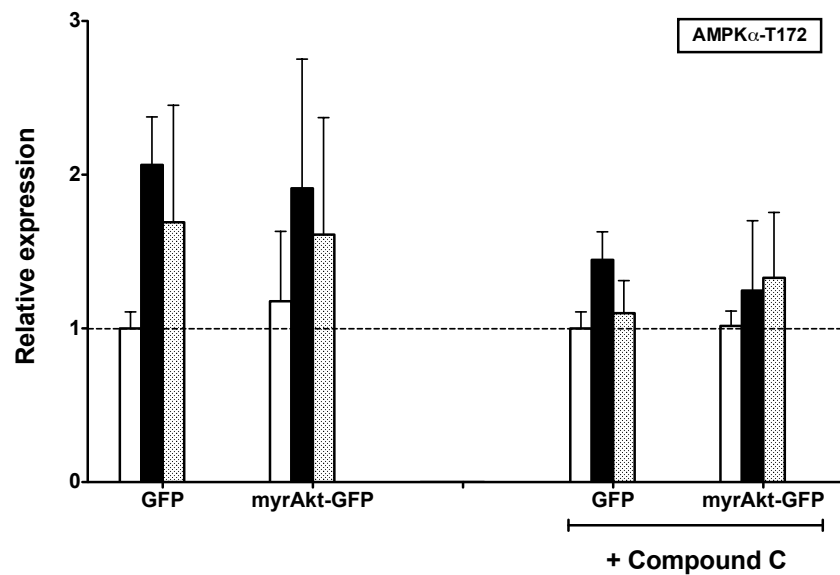


FIGURE 7

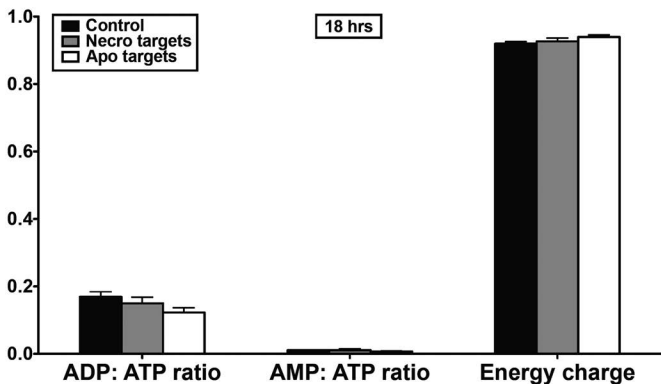
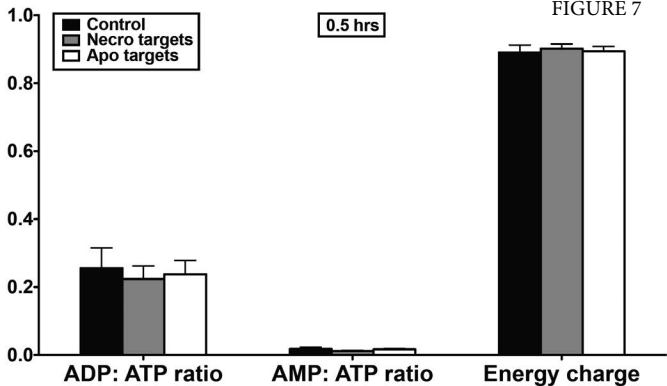


FIGURE 8

